AUS DEM LEHRSTUHL
FÜR INTERVENTIONELLE IMMUNOLOGIE
PROF. DR. PHILIPP BECKHOVE
DER FAKULTÄT FÜR MEDIZIN
DER UNIVERSITÄT REGENSBURG

The role of TSPO in T cell immune control of glioblastoma

Inaugural – Dissertation
zur Erlangung des Doktorgrades
der Medizin

der
Fakultät für Medizin
der Universität Regensburg

vorgelegt von
Marcell-Fabio Kupczyk

2024

AUS DEM LEHRSTUHL
FÜR INTERVENTIONELLE IMMUNOLOGIE
PROF. DR. PHILIPP BECKHOVE
DER FAKULTÄT FÜR MEDIZIN
DER UNIVERSITÄT REGENSBURG

The role of TSPO in T cell immune control of glioblastoma

Inaugural – Dissertation
zur Erlangung des Doktorgrades
der Medizin

der
Fakultät für Medizin
der Universität Regensburg

vorgelegt von
Marcell-Fabio Kupczyk

2024

Dekan:	Prof. Dr. Dirk Hellwig
1. Berichterstatter:	Prof. Dr. Philipp Beckhove
2. Berichterstatter:	Prof. Dr. Hinrich Abken
Tag der mündlichen Prüfung:	22. Oktober 2024

Table of Contents

Zusammenfassung

Das Glioblastom ist der häufigste maligne primäre Hirntumor des erwachsenen Menschen. Weniger als zehn Prozent der Betroffenen überleben die nächsten fünf Jahre und die Gesamtüberlebenszeit nach Diagnosestellung beträgt durchschnittlich 15 Monate. Während innerhalb der letzten Jahrzehnte wesentliche Fortschritte in den therapeutischen Möglichkeiten bei verschiedenen Krebsarten verzeichnet werden konnten, sind die Aussichten für eine vielversprechende Prognoseverbesserung bescheiden. Mit dem Aufkommen der Immuntherapien wurde für die Therapie des Glioblastoms neue Hoffnung geschöpft und einige klinische Studien mit Checkpoint-Inhibitoren durchgeführt. Diese konnten bisher allerdings ebenfalls keine effektive Behandlungsoption darstellen. Deshalb sind fortführende Untersuchungen zu den Immunresistenzmechanismen des Glioblastoms sehr sinnvoll. In dieser Arbeit wird der Einfluss der TSPO-Expression (Translokator Protein 18 kDa) auf die T-Zell-vermittelte Immunreaktion gegen Glioblastomzellen dargelegt. Hauptaugenmerk liegt auf der direkten T-Zell-Krebszelle-Interaktion und auf den von diesen Lymphozyten sezernierten Zytokinen TNFα, IFNγ und TRAIL (TNF-related apoptosis-inducing ligand). Als untersuchte Glioblastomzellen dienten Patientenspenden (BTIC, Flu-T-Zellen und TILs) und die klassischen Glioblastom-Zelllinien U87 und U251. Es wurden Glioblastomzellen und T-Zellen bzw. deren sezernierte Zytokine gemeinsam inkubiert und die Auswirkungen auf die TSPO-Expression untersucht, mithilfe XTT- und Luciferase-basiertem Caspase-3/7-Assay die Rolle von TSPO in der Inhibition der durch die Immunreaktion ausgelösten Apoptose beleuchtet und durchflusszytometrisch die TRAIL-Rezeptorexpression auf den Glioblastomzellen bestimmt. Die Ergebnisse sprechen für eine anti-apoptotische, pro-karzinogene Wirkung des TSPO auf Glioblastomzellen und zeigen zusätzlich, dass die TSPO-Expression durch die Zytokine TNFα und IFNγ verstärkt werden kann. Ebenfalls könnte die pro-apoptotische Wirkung von TRAIL, die durch die Herabregulierung von TSPO verstärkt wird, als Therapie des Glioblastoms Zukunft haben.

Abstract

Glioblastoma multiforme represents the most common type of malignant primary brain tumors in adults. Less than 10 percent of patients live longer than 5 years and overall life expectancy is lowered to 15 months after diagnosis. While research improved the prognosis for some entities of cancer in the last decades, therapeutic advances for GBM generally did not yield promising results. With the advent of immunotherapies, new hope has been raised for the treatment of glioblastoma and clinical trials with checkpoint inhibitors have been conducted. However, these have also failed to demonstrate an effective treatment option to date. Therefore, continued studies regarding immune resistance mechanisms of glioblastoma are needed. In this work, the impact of upregulated TSPO expression (Translocator Protein 18 kDa) on T cell-mediated immune control of glioblastoma is presented. Main focus lies on the direct T cell-cancer cell interaction and on the cytokines TNFα, IFNγ and TRAIL (TNF-related apoptosis-inducing ligand) secreted by these lymphocytes. Patient donor (BTIC, FluT cells and TILs) and classical glioblastoma cell lines U87 and U251 serve as the glioblastoma cells studied. Glioblastoma cells and T cells or their secreted cytokines were incubated together and the effects on TSPO expression were investigated, using XTT- and luciferase-based caspase 3/7 assay to elucidate the role of TSPO in preventing apoptosis triggered by the immune response, and by flow cytometry to determine TRAIL receptor expression on glioblastoma cells. The results support an anti-apoptotic, pro-carcinogenic effect of TSPO on glioblastoma cells and additionally show that TSPO expression can be enhanced by the cytokines TNFα and IFNγ. Likewise, the enhanced pro-apoptotic effect of TRAIL by downregulating TSPO may represent another option for glioblastoma therapy.

1 Introduction

1.1 Glioma and Glioblastoma

Gliomas represent the most common malignant type of primary brain tumors in the central nervous system (CNS) and are categorized in different groups, such as glioblastoma, astrocytoma, oligodendroglioma, ependymoma and other, less common, entities. Originating from neural stem cells, astrocytes and oligodendrocyte precursor cells (OPC), in 70 percent they develop in the supratentorial part of the brain in adults (1,2). World Health Organization (WHO) classifies tumors of the central nervous system by increasing malignancy in grades of I to IV. Most range in grades of WHO I to III, namely pilocytic astrocytoma (I), diffuse astrocytoma (II) and anaplastic oligodendroglioma (III). Glioblastoma multiforme (GBM) is described as WHO IV as this type of astrocytic glioma additionally shows microvascular proliferation, necrosis or both (1). Not only does GBM represent the glioma entity with the highest malignancy, it also is the second most common malignant tumor of the central nervous system and has one of the worst prognoses in the spectrum of cancers. Symptoms often appear, once GBM gained a large size, in form of headaches, nausea, change of personality, memory loss and seizures (3). The development of this full picture usually occurs within a few weeks to months and accordingly leaves little time for fully comprehensive therapeutic measures (1).

Few etiologies are known as causes of glioblastoma. In addition to less common genetic diseases such as neurofibromatosis, Li-Fraumeni syndrome, and tuberous sclerosis, smoking and working in rubber manufacturing are known risk factors (4). However, members of *Herpesviridae* (CMV and HHV6) have also been associated with GBM (5,6). In contrast, the use of cell phones has been ruled out as problematic (7). Circa 90 percent of GBM develop de novo (primary GBM), only 10 percent evolve from low-grade astrocytoma or anaplastic astrocytoma (secondary GBM) (8). In patients older than 50 years, mostly primary GBM are diagnosed, while secondary GBM is more common in younger patients (9). Latter emerges from lower-grade glioma, LGG (WHO II-III) (10).

Therapeutic approaches consist of resection of the tumor, as well as radiation-, chemo- and immune therapy. Primarily, MRI is used to detect glioblastoma and plan further interventions. If the tumor is located inconveniently or the CNS is multifocally affected, stereotactic biopsy is performed for histopathologic evaluation. Surgical (partial) removal of glioblastoma is often performed with 5-ALA (5-aminolevulinic acid) given perorally beforehand to distinguish healthy brain tissue from tumor tissue, as the latter converts the drug more intensely and thus becomes visible as stronger fluorescence (3,11).

In the therapeutic course, radiation therapy (RT) or radio-chemotherapy is the next step. Here, the cranium is irradiated with 30 x 2 Gy = 60 Gy while 75 mg/m² of temozolomide (TMZ) are administered concomitantly. However, depending on the patient's condition, radiotherapy can be dispensed with and TMZ can be given exclusively (3). TMZ is the leading chemotherapeutic agent in treatment of GBM. It alkylates N^7 and O^6 of the guanine bases in DNA, causing apoptosis through DNA damage. TMZ was proven to suppress tumor growth, but circa 55 percent of patients hold a resistance and almost every patient develops the latter during chemotherapy. Decisive reason for this is found to be the O^6-methylguanine-DNA methyltransferase (MGMT) repair system, which removes methyl- and alkyl residues from the DNA, thus impairing the efficacy of TMZ (12). Therefore, patients ≥ 65-70 years with GBM are screened for MGMT methylation, which shows a sensitivity for TMZ as methylated MGMT is inactive in its DNA repair function. If MGMT is unmethylated at this older age, administration of TMZ is omitted and hypofractionated radiotherapy with 15 x 2,66 Gy = 40 Gy follows. Therapy including surgery, administration of TMZ and RT is summarized as Standard of Care (SOC) (3).

The prognosis for GBM patients is unfavourable. Circa 2,6 percent live longer than 10 years and mean overall survival is lowered to 15 months after diagnosis. Patients with secondary GBM experience 31 months of average survival (10). In comparison, pilocytic astrocytoma (WHO I) survival rate after 10 years ranges at 90 percent, WHO II tumors between 37 and 62 percent and WHO III at around 19 to 39 percent. (1).

Since lymphocytes proliferate strongly in a situation-adapted manner, they are very susceptible to DNA damage and corresponding apoptosis. TMZ can therefore lead to a relevant lymphopenia, and this effect is further enhanced by radiotherapy. Nevertheless, TMZ enhances anti-tumor effect of immune cells in human studies (12) and usage of TMZ in a therapy regimen averagely enhances the survival of the patient by 2 to 3 months (13). Despite optimal care glioblastoma has a high rate of recurrence (14). Therapy of the recurrent GBM consists of, if possible, further surgery, once again administration of TMZ and, different to newly occurring GBM, also administration of the alkylane Lomustine and the VEGF-antibody Bevacizumab (3,15).

1.2 Immune resistance mechanisms in Glioblastoma

As “multiforme” implies, GBM behaves heterogeneously in macroscopic (necrosis, haemorrhage, cystic and gelatinous areas), microscopic (microvascular proliferation, pseudo-palisading necrosis) and genetic aspects (16). It presents a diverse distribution of genetic aberrations among the cells in the tumor (17,18). Using these differences, GBM is classified into proneural, classical or mesenchymal subtypes. Earlier theories included the neural type as well, which existence remains controversial (19). While mutations in PDGF-RA, TP53 and IDH are common for the proneural type, mutations of EGFR and NF1/TP53 stand for the mesenchymal and classical types (20). Secondary glioblastoma carries a mutation in IDH (IDH^{mut}), which causes an increment in production of cell-damaging reactive oxygen species (ROS) (21), contributing to the better prognosis of the secondary type. Another reason for the better outcome in patients with this entity developed from LGG lies in its classification as proneural, while primary, IDH^{wt}, GBM can develop from all three subtypes. Mesenchymal and classical GBM show the poorest prognoses (16,20). In multiple cases, subtype status changes in recurring GBM, here, proneural-mesenchymal-transition (PMT) resembles tumor progression (19) similar to the epithelial (EMT) in other cancers (22). Loss of heterozygosity (LOH), which often appears in GBM, enhances the tumorigenic potential of GBM by partial inactivation of Apaf-1 and thereby negatively regulates p53-mediated apoptosis (23). GBM cells especially express higher levels of Indoleamine 2,3-Dioxygenase (IDO) than LGG, correlating with poor prognosis (24).

In addition to molecular alterations, glioblastoma multiforme has developed several strategies to evade the immune system, which further contributes to therapy resistance.

1.2.1 Immune Tumor Microenvironment (iTME)

The blood-brain barrier (BBB) preserves the homeostasis of the CNS, by endothelial tight junctions and a set of drug efflux pumps, through excretion of cytokines PGE_2, and IL-10, both influencing intercellular matrix, and TGFβ, restricting regional immune responses (25). But, contrary to earlier hypotheses, the brain is not an immune privileged organ, as it maintains a high level of interaction with the immune system (26) and even a lymphatic system was discovered to be involved in the CNS. A few years ago, it was demonstrated that the CNS is connected to deep cervical lymph nodes, T cells and antigens circulate between these and the cerebrospinal fluid (CSF)-containing perivascular space. This mechanism overcomes the blood-CSF-barrier, enabling the recognition of tumor cells in the CSF as well (27). Integrity of the blood-brain-barrier is reduced in inflammatory states, allowing increased interaction of the

CNS with the lymphatic system (25), yet still poses an immense problem for bioavailability of chemotherapeutics (28). GBM maintains an immunosuppressive tumor microenvironment to promote expansive growth while evading interaction with immune cells. Tumor associated macrophages (TAM), also referred to as microglia, in the Immune Tumor Microenvironment (iTME) are involved in the immune response against glioblastoma, which are classified into M1 (pro-inflammatory) and M2 (anti-inflammatory) microglia. This distinction can be made under in vitro conditions, with macrophages ranging on a spectrum of different immune activities (10). These two types can be distinguished by their different protein expression: CD86, co-stimulator in the T cell-APC synapse (29), IL-1β and TNFα represent the M1 type, CD206 (mannose receptor) (30), IL-10 and TGFβ represent the M2 type (31). M1 macrophages are stimulated by IFNγ, M2 by immunosuppressive cytokines such as IL-4, -10, -13 (10,32). In the iTME, enrichment of immunosuppressive regulatory T cells (Tregs) and neutrophil-activating Th17 cells is controlled context-dependent regarding other immune cells and microenvironmental stimuli like cytokines. GBM is capable of shifting between Treg and Th17 prevalence (33), whereas latter induces chronic inflammation, interestingly contributing to tumor expansion (25). Apart from the iTME, GBM expresses ligands on its cell surface to escape the immune system.

1.2.2 PD-L1/PD-1 expression in GBM

One of the several reasons for the immune evasive capability of GBM is the expression of immunosuppressive Programmed Death-Ligand 1 (PD-L1) on tumor cells. PD-L1 (CD274) interacts with its receptor Programmed Death 1 (PD-1) on T cells and triggers SHP-2 phosphatase to be recruited to the cytoplasmic immunoreceptor tyrosine-based switch motif (ITSM) domain of PD-1. (34,35). This interaction causes T-cell dysfunction by decreasing the production of cytokines and cytotoxic molecules and by increasing the expression of pro-apoptotic genes in the cytotoxic T-cells (35). The PD-L1/PD-1 axis promotes generation of Treg by maintaining the expression of Foxp3 (36), impairs T-cell function and induces apoptosis in T cells, therefore restraining autoimmunological reactions (12,25). PD-1 is highly expressed by activated T cells and causes a negative regulation of the immune response by interacting with overexpressed PD-L1 on glioblastoma cells and microglia (25). TMZ upregulates PD-L1 (37), but even though more than 88 percent of newly diagnosed and 72 percent of recurrent GBM express PD-L1, this has neither positive nor negative effect on survival (12,38). Other initiators of PD-L1 expression are interferon gamma (IFNγ) and tumor necrosis factor alpha (TNFα). IFNγ binds to its receptors IFNGR1 and IFNGR2 and activates

PD-L1 mRNA transcription via Interferon regulatory factor 1 (IRF1) involving the JAK/STAT-axis (38). NF-kB-induced CSN5 inhibits ubiquitination and thus degradation of cytosolic PD-L1 (39,40). Toll-like receptors (TLR) are evolutionary well conserved receptors which recognize pathogen-associated molecular patterns (PAMPs) and initiate an immune response. In the iTME of GBM, heat shock proteins released by tumor cells function as agonists, mimicing those molecular motifs originating from microbes. Via My88-pathway, PD-L1 transcription in the GBM cells is enhanced, contributing to immune resistance (25,40).

1.2.3 TRAIL resistance

TRAIL (TNF-related apoptosis inducing ligand) is a pro-apoptotic cytokine and is able to trigger apoptosis by binding to death receptors TRAIL-R1 (DR4) and TRAIL-R2 (DR5). The homotrimerized TRAIL/TRAIL receptor-complex recruits FAS-associated death domain protein (FADD) and further pro-caspase 8, forming the death-inducing silencing complex (DISC) (41). Through ubiquitination, caspase 8 aggregation at the DISC is enhanced. DISC cleaves pro-caspase 8 allowing activated caspase 8 to cleave caspase 3, initiating extrinsic apoptosis. Caspase 8 also causes direct execution of apoptosis by mitochondrial cytochrome c release after initiating the formation of pores in the outer mitochondrial membrane (41). One important regulatory mechanism consists of the caspase 8 homologue c-FLIP (FLICE-like inhibitory protein). c-FLIP competes with caspase 8 for binding to FADD, but is not capable of cleaving caspase 8. Consequently, c-FLIP is found to be upregulated in cancers as a resistance mechanism (42). GBM resists pro-apoptotic modulation by TRAIL. It has been discussed as a promising therapeutic pathway for decades (43), as it shows effect on a wide spectrum of tumors and exerts no cytotoxicity in healthy cells (41). TRAIL-R expression is not detectable in healthy brain tissue, while TRAIL-R1/-R2 are expressed on glioblastoma cells, and, contradictory, even higher in cells with higher malignancy. TRAIL-R3/-R4 are decoy receptors and are expressed on oligodendrocytes and neurons, functioning by competing for their cognate ligands like TRAIL, effectively decreasing its concentration at TRAIL-R1/-R2. TRAIL-R expression of tumor cells and survival are positively correlated. Elevated expression of TRAIL-R3/-R4, decreased expression of TRAIL-/TRAIL-R downstream proteins like Caspases and FADD and overexpression of c-FLIP contribute to the intrinsic TRAIL resistance of glioblastoma cells (44,45). Radiation (46) and chemotherapy (47) can cause an upregulation of TRAIL receptors, resulting in an intensified cytotoxic effect of TRAIL (44).

1.3 Clinical trials of immune checkpoint inhibitors and concepts in GBM therapy

In the last decades, immune therapies have been showing an immense rise in treatment of different types of cancer such as melanoma (48), NSCLC (49) and lymphoid malignancies (50) but in the case of GBM, effectiveness of immunotherapeutic options is still insufficient (20). One well-studied option is immune checkpoint inhibition (ICI), mediated by the administration of monoclonal antibodies against, for instance, PD-1, PD-L1 or CTLA-4. In melanoma, Nivolumab and Pembrolizumab (anti-PD-1) have been proven as effective. In combination with anti-CTLA-4 monoclonal antibody Ipilimumab a response rate of 47 percent in melanoma was observed (12). CTLA-4 binds CD80/86 to negatively regulate co-activation during MHC-TCR interaction (51). While PD-1 inhibitors showed high response rates of 87 percent in patients with Hodgkin's lymphoma, cancers of solid organs like GBM are less affected by this new therapeutic strategy with percentages ranging between 15-40 (34).

For PD-1-inhibitors, three major phase III studies with antibodies recently failed. CheckMate 143 (NCT02017717) was a multicentric, randomized trial in phase III and compared 369 relapsed patients with GBM. Patients were randomized 1:1 to a treatment with Nivolumab (anti-PD-1-ab) or Bevacizumab (anti-VEGF-ab). The primary endpoint, improved mean overall survival (mOS), was not reached, as the effects were comparable with 9,8 months for patients treated with Nivolumab (95% CI, 8,2-11,8) and 10,0 months for patients treated with Bevacizumab (95% CI, 9,0-11,8). (34,52). CheckMate 498 (NCT02617589) was a multicentric, randomized trial in phase III and compared 560 newly diagnosed patients (in comparison to recurrent GBM in CheckMate 143) with MGMT-unmethylated GBM. Patients were randomized 1:1 to a treatment with Nivolumab and radiation therapy (RT) or TMZ and RT. The primary endpoint, improved mean overall survival (mOS), was not reached, with 13,4 months for patients treated with Nivolumab + RT (95% CI, 12,62-14,29) and 14,88 months for patients treated with TMZ + RT (95% CI, 13,27-16,13) (53). The third major multicentric, randomized trial in phase III, CheckMate 548 (NCT02667587), compared Nivolumab and SOC with placebo and SOC in 693 patients with newly diagnosed, MGMT-methylated (in opposition to CheckMate 498) GBM. Usage of Nivolumab did not increase mOS with 28,9 months (95% CI, 24,4-31,6) for Nivolumab and 32,1 months for SOC (95% CI, 29,4-33,8) (54,55).

One reason for failure of therapy was described as radiation therapy-induced lymphopenia and, similar to TMZ, radiation affects rapidly proliferating cells as well (55). Other adverse effects of ICI themselves are electrolyte changes and fluctuations in cell counts, but also autoimmune disorders of the kidneys and adrenal glands, liver, lungs, pituitary gland and intestines, which

take a long time to treat; there is also an increased risk for development of type 1 diabetes mellitus (56).

Therapeutic effect of Ipilimumab in recurrent GBM was examined in a phase I study for tolerability and safety. Combination of Ipilimumab and Nivolumab generated more adverse effects than Nivolumab alone. This potentially emerges from the involvement of CTLA-4 in the early activation of T cells as it promotes the CD28-CD80/86-co-stimulation (55).

1.4 Translocator protein (TSPO)

1.4.1 Characterization of TSPO and its role in Glioblastoma

Over four decades ago, another benzodiazepine-binding site outside of the CNS was found. To differ this new receptor from known GABA, which acts in the CNS and was therefore called central-type benzodiazepine receptor (CBR), it was analogously named PBR for peripheral-type benzodiazepine receptor. PBR was discovered to consist out of VDAC, voltage-dependent anion channel (32 kDa), ANT, adenine nucleotide transporter (30 kDa) and IBP, isoquinoline-binding protein (18 kDa). As nomenclature was not used consistently among the research groups, IBP was renamed 'Translocator Protein 18 kDa' (TSPO) (57). The complex of TSPO, VDAC and ANT is located in the mitochondria. Here, ANT forms a channel in the inner mitochondrial membrane (IMM) and is connected to VDAC in the outer mitochondrial membrane (OMM). TSPO is an evolutionary well conserved, highly hydrophobic protein complex with five alpha-helical transmembrane domains (58), and is found in a wide variety of other animals (57). The complex of TSPO, VDAC and ANT serves several important functions in cell biology, such as transport of cholesterol and therefore is involved in steroid synthesis and regulation of apoptosis (20). TSPO also prevents the accumulation of Protoporphyrin IX (PPIX) (59), which causes erythropoietic protoporphyria in patients with ferrochelatase-deficiency (60). As its knockout causes embryonic death in mice, TSPO seems to be involved in vital cell functions (57). TSPO is expressed by microglia, endothelial cells, pericytes and tumor cells in GBM tissue (61).

Currently, TSPO is primarily used as a biomarker for diagnosis and prognosis of brain lesions in PET-Scans. TSPO serves this role remarkably as it is hardly detectable in healthy brain tissue, but up to 15 times higher in glioma cells and its expression positively correlates with malignancy (62). Several studies have shown that upregulated TSPO also correlates with a higher rate of proliferation, worse prognosis and lower life expectancy (17).

A variety of TSPO ligands was developed. However, the pharmacodynamics of TSPO ligands such as PK 11195, Ro5-4864, DPA-714 and FGIN-127, are discussed controversially as their role as agonists or antagonists is not clear (58). In PET imaging, [^{11}C]PK11195, TSPO antagonist (17,63), is frequently used and displays increased activity in neurodegenerative diseases, stroke and in traumatic brain injury (64,65). PK 11195 yields a 2-fold higher detection rate in glioma in the first trial, and astrocytoma of low grade was able to be differentiated from gliomata that were showing characteristics of GBM. But, PK 11195 is not ideal as it possesses a low bioavailability (17). [^{18}F]DPA-714 was shown to be at least equivalent to distinct neuroinflammatory states (66), as the former exhibits a higher nonspecific binding and shorter half-life (20 minutes) (67). Ro5-4864, another PET tracer, on the other hand is classified as TSPO agonist (68).

Downregulation of TSPO causes a lower oxygen metabolism, lower ATP levels, and takes part in the modification of fatty acids in production of steroidogenic hormones. It is involved in the generation of ROS and restrains mitochondrial autophagy, following a lower rate of ubiquitination in the cell (58). Also, TSPO has an effect on the invasiveness of GBM. Application of PK 11195 or a knockdown of TSPO in U118 GBM cells led to a decreased adhesion to extracellular matrix and as genes coding for adhesional mechanisms are downregulated and TSPO is found to be translocated to the nucleus, it might affect cells at a genetic level (17,69).

Proliferative effects were described for TSPO: in rat glioma, TSPO upregulation correlated with higher rate of proliferation and in a human astrocytoma cell line, lower TSPO levels were observed together with lower ability of proliferation. As TSPO ligands affect biosynthesis of steroid hormones, changes in rate of proliferation may be achieved by influencing TSPO (17).

1.4.2 Role of TSPO in apoptosis

As mentioned in the previous section, TSPO is of high importance for essential cell functions. The mitochondrion holds an essential role in apoptosis and with TSPO located in the OMM, it is able to exert regulative functions in programmed cell death. During the late stage in apoptosis, mitochondrial permeability increases via opening of the mitochondrial permeabilization transition pore (mPTP). Consequently, cytochrome c is released and the caspase cascade would be initiated or continued. TSPO may be a part of this pore and could regulate its opening, thus alleviating resistance caused by Bcl-2 (17). The Bcl-2 family consists of several anti-apoptotic members like Bcl-2 itself, while pro-apoptotic Bax enhances mitochondrion-linked apoptosis

(70). Likewise, mPTP may be important for the treatment of traumatic brain injury with etifoxine, a nonbenzodiazepine anxiolytic and TSPO ligand (71). However, there are controversial reports on the involvement of TSPO in mPTP (20). Competition for the TSPO-binding site blocks its apoptotic effects. For example, the pro-apoptotic effect of glutamate is not exerted when TSPO is downregulated. PK 11195 reduces anti-apoptotic effects of Bcl-2. While many different ligands cause mitochondrial membrane permeabilization, cytochrome c release and apoptosis, the binding site of the ligand is crucial to its impact as it was shown that the TSPO ligand Ro5-4864 binds differently and has no effects on apoptosis (17). TSPO downregulation directly lowered apoptosis rate, while PK 11195 induced apoptosis in neuroblastoma and leukemia cells. Collapse of the mitochondrial membrane potential causes apoptosis via the caspase system. Off-target effects of TSPO ligands also have to be taken into consideration as PK 11195 and Ro5-4864 cause opposing effects in case of apoptosis (20).

2 Aim of the thesis

Glioblastoma is considered one of the most malignant tumors and has a poor prognosis. Recent developments in immunotherapeutic strategies hold promise. However, due to the poor clinical efficacy of these approaches, further possibilities and causes of therapeutic resistance are being investigated. GBM has evolved several mechanisms such as expressing immune checkpoint inhibitors and thereby evade the immune system. At the same time, GBM upregulate the expression of the mitochondrial protein TSPO. In my thesis I aim to investigate the role of TSPO in T cell immune control of glioblastoma. To this end, I used co-culture models of primary glioblastoma cells of different subtypes and assessed the quantity of TSPO-mRNA following treatment with cytotoxic T cells (FluTC and tumor-infiltrating lymphocytes (TILs)) or supernatant of activated T cells. Next, I determined the main T cell derived agents responsible for TSPO upregulation by blocking the effects of the cytokines TNFα and IFNγ. Then, I measured TRAIL expression and secretion of T cells in increasing states of activation to estimate the level of potential TRAIL concentrations in vivo. Further, I determined Fas, DR4 and DR5 expression on classical glioblastoma cell lines U87 and U251 to elucidate their susceptibility to T cell attack and TRAIL. Finally, I downregulated TSPO expression in U87 and U251 cells by using TSPO-specific siRNAs and study the effects on T cell- or TRAIL-mediated cytotoxicity and activation of the caspase cascade as indicators for enhanced apoptotic activity, in order to present TSPO as a relevant protagonist in immune resistance of GBM.

3 Results

3.1 Correlation between the expression of *TSPO* and T cell markers or TNF/IFNγ receptors in GBM

To find out whether *TSPO* expression in glioblastoma correlates with T cell infiltration, TCGA-GBM data was analyzed using GEPIA webserver. Correlation between *TSPO* mRNA expression and expression of T cell marker genes are displayed in Figure 1. The R for correlation between *TSPO* values at R = 0,32 for *CD3E*, R = 0,38 for *CD4*, R = 0,24 for *CD8A*, R = 0,31 for *Granzyme B* and R = 0,23 for *Perforin 1*. The results show that the *TSPO* gene and all studied T cell markers are positively correlated. Additionally, *TSPO* expression positively correlated with *IFNGR1*, *TNFSF1A* and *TNFRSF1B* expression in GBM.

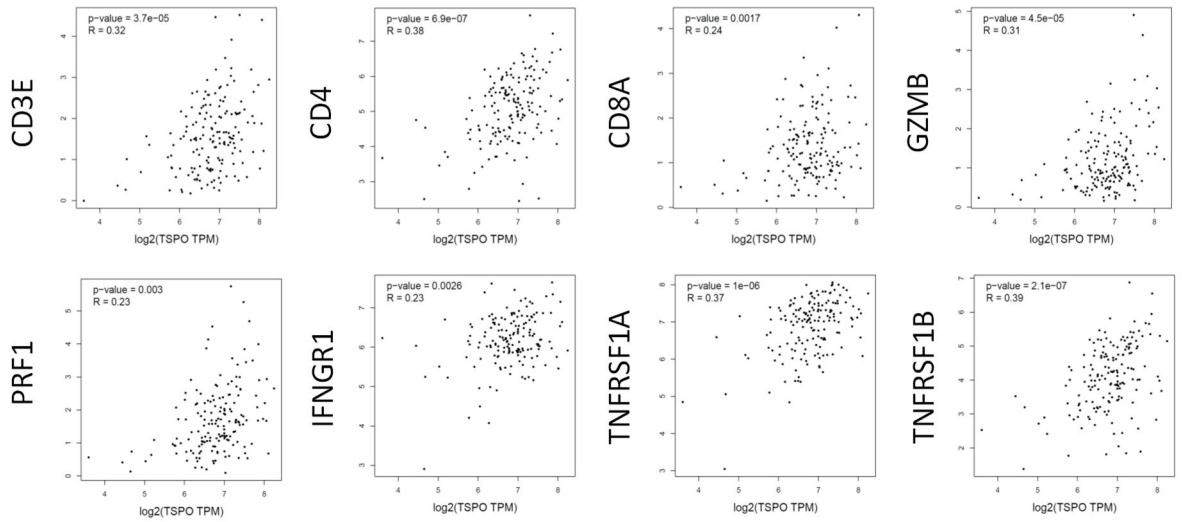

Figure 1: Correlation between *TSPO* gene and genes of immune relevant agents. Pearson correlation of *TSPO* gene and *CD3E*, *CD4*, *CD8A*, *GZMB*, *PRF1*, *IFNGR1*, *TNFRSF1A* and *TNFRSF1B* genes in TCGA-GBM dataset. Log scale was used for visualization and non-log scale for calculation, counts in transcripts per million (TPM). All results are significant as $p < 0,05$. Results taken from *gepia.cancer-pku.cn.*

3.2 Co-culture of glioblastoma cells and FluTC

To investigate the role of TSPO in cytotoxic T cell-mediated killing of glioblastoma cells, I used an *in vitro* co-culture model where I set primary or classical glioblastoma cells as target cells for Influenza (Flu) antigen-specific CD8+ T cells (FluTC). These react specifically to the Flu-antigen (Flu-peptide). Flu antigen is added to the HLA-A2+ tumor cells in order to replace self-peptides presented on HLA-A2 molecules. When the TCR of the FluTC recognize the Flu-antigen loaded HLA-A2, FluTC then secrete cytotoxic effector molecules like Perforin and

Granzyme B, TNFα and IFNγ (Figure 2A). To generate FluTC, my supervisor isolated CD8+ T cells from peripheral blood mononuclear cells (PBMCs) of an HLA-A2 positive donor and expanded them antigen specifically with Flu peptide and low dose IL-2 and IL-15. Subsequently, I FACS-sorted FluTC using FACS pentamer staining and expanded CD8+/Pentamer+ cells in the presence of CD3 antibody and IL-2 (Figure 2B). FluTC were expanded by 200-fold and FACS analysis displayed circa 80 percent of live lymphocytes are both positive for CD8 and Flu-specific TCR.

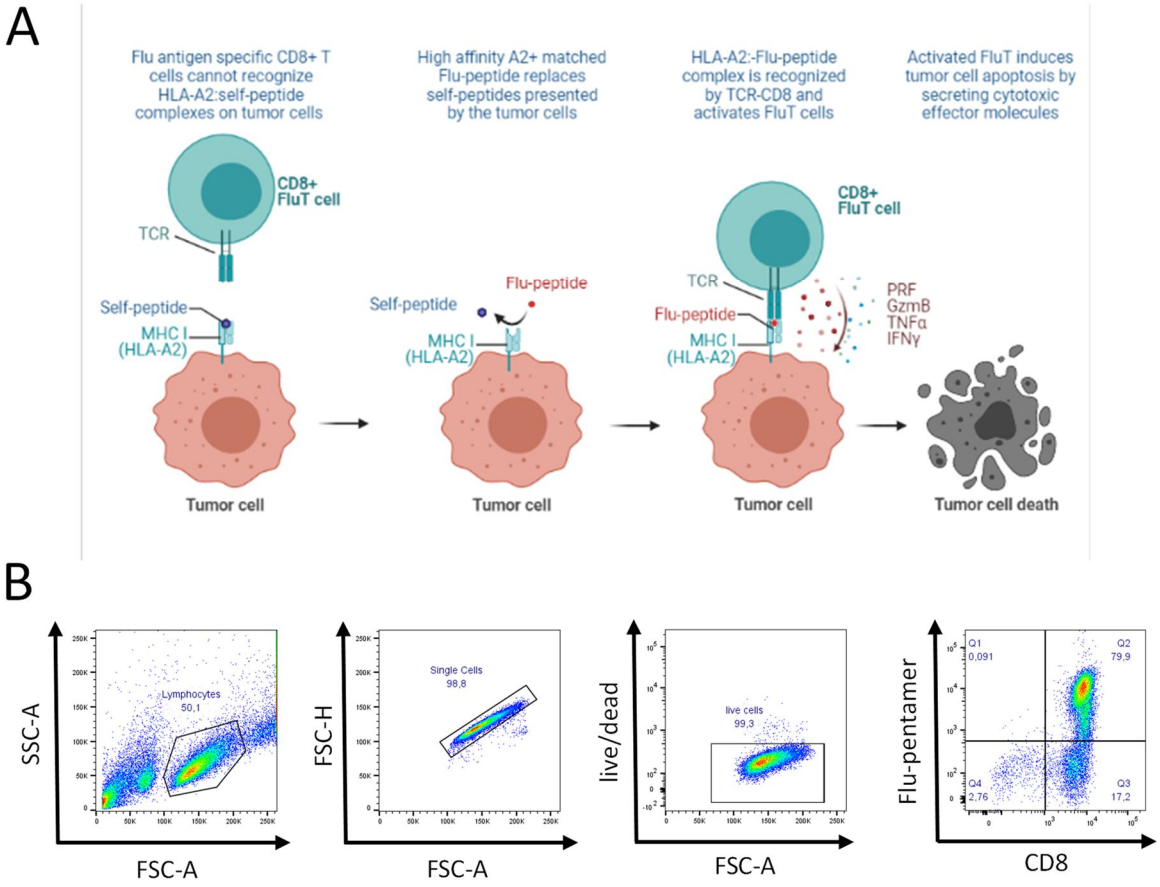

Figure 2: Co-culture of HLA-A2+ tumor cells and CD8+ FluTC and FACS analysis of FluTC. **(A)** FluTC kill tumor cells by secretion of Perforin, Granzyme B, TNFα and IFNγ after recognizing high affinity Flu-peptide presented by HLA-A2. Scheme was generated by my supervisor Ayse Nur Menevse using BioRender.com. **(B)** FACS analysis of Flu-pentamer and CD8 antibody-stained T cells after expansion. All samples were gated on lymphocytic, single, live cells.

3.3 Impact of T cells and T-cell derived cytokines on TSPO expression in BTICs

To analyse if TSPO expression can be upregulated in glioblastoma cells when they encounter immune effector cells like FluTC or by their secreted effector molecules, I set up co-culture experiments using primary glioblastoma cell lines BTIC13 (mesenchymal type) and BTIC129 (proneural type). Both cell lines were treated with supernatant of activated T cells to measure the effect of e.g. cytokines secreted by activated cytotoxic T cells on TSPO expression. Since BTIC13 and BTIC129 were identified to be HLA-A2 positive, experiments with FluTC were possible. They were pulsed with Flu peptide in concentrations of 0,001 µg/mL, 0,0001 µg/mL and 0,00001 µg/mL and then co-cultured with FluTC in the same amount as the tumor cells to observe the effects of antigen-specific cell killing on the TSPO expression.

Control medium (CLM) was used to monitor the basal level of TSPO expression in BTICs. After 24h incubation the cells were collected and TSPO mRNA expression was analysed by real-time qPCR (Figure 3A-3B). The results revealed a 2-3-fold induction of TSPO mRNA by treatment with activated supernatant of FluTC in both cell lines and treatment with supernatant of activated TIL129 in BTIC129. Treatment with Flu peptide in concentrations of 0,001 µg/mL and 0,0001 µg/mL induced TSPO expression in BTIC13 and BTIC129 while upregulation was lower for the cells treated with a lower concentration of Flu peptide. The lowest peptide concentration in BTIC13 and the TIL129-treated BTIC129 did not cause an induction.

Because the results of this experiment showed T cell mediated upregulation of TSPO expression, we speculated whether TNFα and IFNγ secreted by T cells are responsible for this phenotype. First of all, ELISA was performed to quantify the amounts of TNFα and IFNγ in the co-culture media that was collected together with the treated BTIC13 and BTIC129 cells that were analyzed in Figure 3A-3B (Figure 3C-3F).

Both cytokines were not detected in the samples pulsed with 0,00001 µg/mL Flu peptide and in the sample with tumor cells alone (CLM). 8 ng/mL of TNFα and 110 ng/mL of IFNγ were detected in the supernatant of activated FluTC for BTIC13, 3 ng/mL of TNFα and 120 ng/mL of IFNγ for BTIC129 samples. In the supernatant of the sample pulsed with 0,001 µg/mL Flu peptide and FluTC 0,6 ng/mL of TNFα and 3 ng/mL of IFNγ for BTIC13 and 0,04 ng/mL TNFα and 3 ng/mL of IFNγ were detected. The supernatant of the sample treated with 0,0001 µg/mL and FluT shows, with 0,1 ng/mL TNFα and circa 1,5 ng/mL IFNγ for BTIC13 and no detected TNFα and 0,1 ng/mL IFNγ for BTIC129, less cytokines than the supernatant of the sample treated with the next higher concentration. For the co-culture samples of BTIC129 with TIL129

9 ng/mL of TNFα and 150 ng/mL of IFNγ were detected (Figures 3E-3F). A microscopically visible higher cytotoxic effect in the wells treated with the highest concentration of Flu peptide was observed just before the cells were detached for analysis.

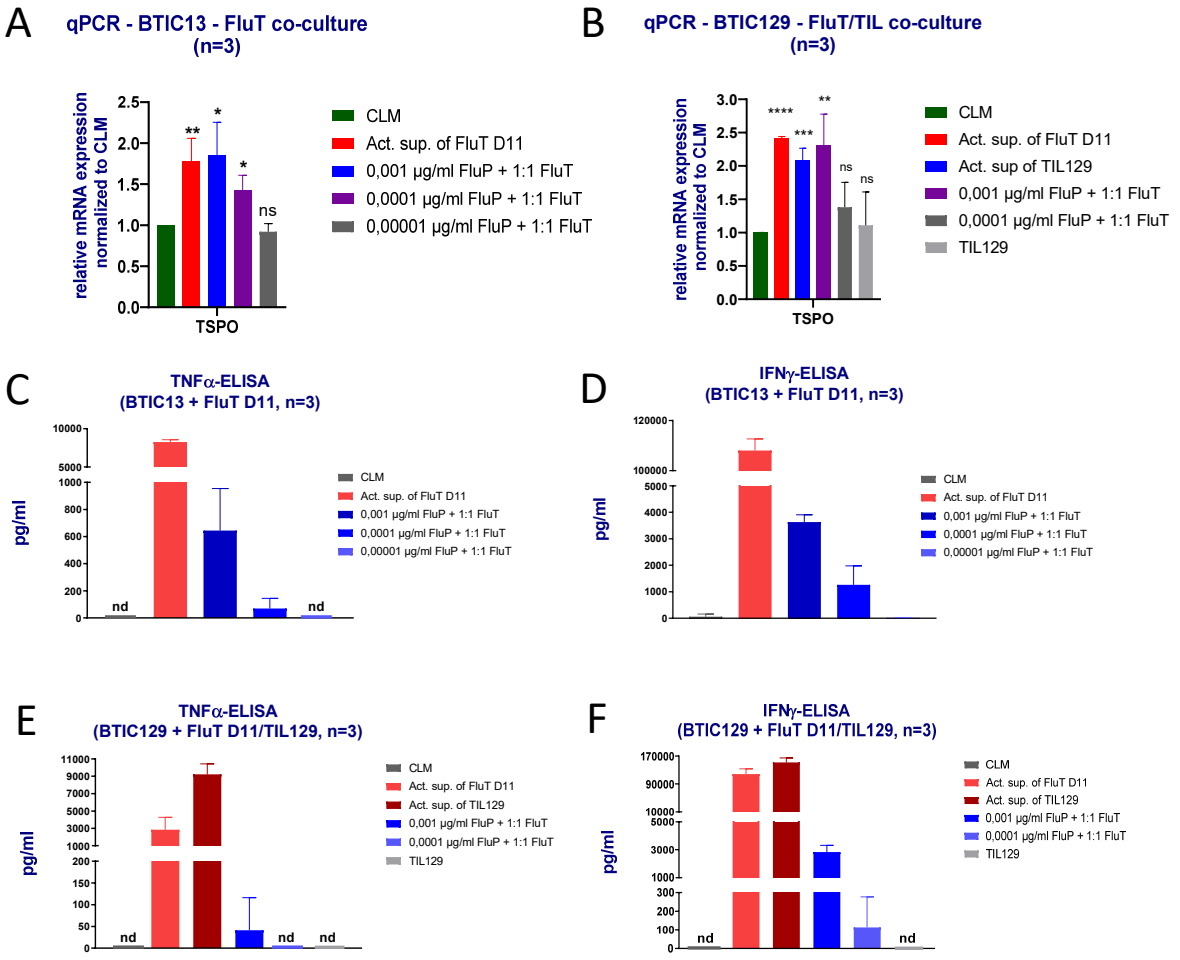

Figure 3: Impact of T cells and T-cell derived cytokines on TSPO expression in BTICs. (A) BTIC13 were treated for 24h either with only activated supernatant of FluT D11 cells or were pulsed for 1h with Flu peptide in varying concentrations and then co-cultured with 1:1 FluT D11 cells. **(B)** BTIC129 were treated for 24h with activated supernatant of FluT D11, activated supernatant of TIL129, TIL129 cells, or were pulsed with two different concentrations of Flu peptide for 1h and were then co-cultured with 1:1 FluTC. **(A-B)** CLM was used as a control. mRNA expression of TSPO was analysed by qPCR. Three independent experiments were compiled and TSPO expression was normalized to CLM treated cells. **(C-F)** Compiled results of three independent ELISA for TNFα and IFNγ of (C-D) BTIC13 experiments, (E-F) for BTIC129 experiments. Cell media of the differently treated BTIC13 and BTIC129 samples analysed for TSPO expression were collected 24h after the co-culture/treatment. For each sample duplicates were analysed, except for the third sole experiment of BTIC13, where triplicates were used. No cytokines were detected in the CLM sample and the sample with lowest concentration of Flu-peptide. Error bars indicate +/- SD. P-values were calculated using two-tailed paired student's t-test. * = $p < 0.05$, ** = $p < 0.01$, *** = $p < 0.005$, **** = $p < 0.001$. The experiment for TSPO induction in BTIC13 was performed by technical assistants Nicole Heuschneider and Jasmin Mühlbauer.

3.4 Impact of TNFR/IFNGR blockade on TSPO and PD-L1 expression in BTICs

After showing that TNFα and IFNγ levels correlate with TSPO expression in BTIC13 and BTIC129, I investigated if TSPO expression is ultimately upregulated by TNFα and IFNγ or by other factors secreted by immune cells as well (Figure 4). Thus, neutralizing antibodies were added to the supernatant of activated FluTC to bind TNFα and IFNγ, to eliminate the effect of these cytokines on any potential modulation of TSPO expression in BTIC13. These were seeded and treated one day later with TNFα- and/or IFNγ-neutralized supernatants. Supernatant was incubated for 2h either with anti-TNFα-, anti-IFNγ- or both antibodies. IgG treated supernatant was used as control and plain CLM to measure the basal level of TSPO and PD-L1-expression.

To determine which concentration of neutralizing antibody works most efficiently, the supernatant of activated FluTC was incubated for 2h with concentrations ranging from 0,625 µg/mL to 20 µg/mL, followed by ELISA to measure the concentrations of the TNFα and IFNγ that could not be neutralized (Figure 4A-4B). Analysis revealed that no TNFα was detected in the supernatants treated with any tested concentration, while IFNγ was reduced by circa 60%, independent of the amount of added anti-IFNγ-AB. Because these results prove all tested concentrations of antibodies as equally efficient, 2,5 µg/mL was set as the working concentration in the supernatants used for the setup where BTIC13 were to be treated with various cytokine-depleted supernatants. Cells were co-cultured with the AB-treated supernatants for 24h, then cell medium and cells were collected. Cell pellets were analysed by qPCR for mRNA expression of TSPO and PD-L1 (Figure 4E). PD-L1 expression acted as a positive control as it is known to be upregulated if TNFα and IFNγ bind to the cellular receptor (8). In the sample treated with IgG-incubated supernatant TSPO expression increased by 2,5-fold and PD-L1 expression by 10-fold compared to the cells exposed to CLM. Neutralization of one cytokine alone induced TSPO expression by circa 2-fold and PD-L1 expression by 5-fold, both antibodies together resulted in a 40 % induction in TSPO and 4-fold induction in PD-L1 expression in comparison to CLM. Supernatants were analyzed by ELISA for remaining cytokines (Figure 4C-4D). While TNFα was not detectable in the samples treated with anti-TNFα-antibody, anti-IFNγ-antibody treated samples contained circa 40 % of IFNγ in comparison to control. These findings are similar to the results of the experiment depicted in Fig. 4A-4B.

Because the expression levels of the CLM-treated and anti-TNFα and anti-IFNγ treated cells were not even, therefore not supporting the hypothesis that TNFα and IFNγ are the ultimate mediators of TSPO upregulation, another way to neutralize the effects of these cytokines on

BTIC13 was used. Here I treated the cells with either anti-TNF-R1-, -R2-, IFNG-R1- or all three antibodies in order to fully block any effect of both cytokines. BTIC13 were seeded and incubated on the next day with the respecting set of blocking antibodies for 30 min prior to supernatant treatment. For basal TSPO expression CLM treated cells were included as a control. After 24h incubation, TSPO expression was analysed by qPCR (Figure 4F). Supernatant treatment in IgG-incubated cells induced TSPO expression by 2,5-fold and PD-L1 expression by 10-fold. Treatment with anti-TNF-R1 antibody resulted in an induction by 2-fold of TSPO- and by 5-fold in PD-L1 expression, with anti-IFNG-R1 antibody in an induction of 25% in TSPO- and 2,5-fold in PD-L1 expression compared to basal level. Treatment of supernatant with all three antibodies completely abrogated supernatant-induced TSPO and PD-L1 expression as their expression was measured to be the same in the cells treated with CLM. Treatment with anti-TNF-R2 antibody showed a similar TSPO expression as incubation with IgG and for PD-L1 an even higher value than IgG. The experiment was repeated with BTIC129 (Figure 4G). Supernatant treatment in IgG-incubated cells induced TSPO and PD-L1 expression similarly to the results with BTIC13. Treatment with anti-TNF-R1 antibody resulted in an induction of TSPO expression to the same level as IgG treatment and increased by 7-fold in PD-L1 expression, with anti-IFNG-R1 antibody in an induction of 2-fold in TSPO- and 5-fold in PD-L1 expression compared to basal level. Treatment of supernatant with all three antibodies resulted in an increase of 66% in TSPO expression and 4-fold in PD-L1 expression compared to the cells treated with CLM. Treatment with anti-TNF-R2 antibody showed an even higher value for TSPO and PD-L1 expression than IgG.

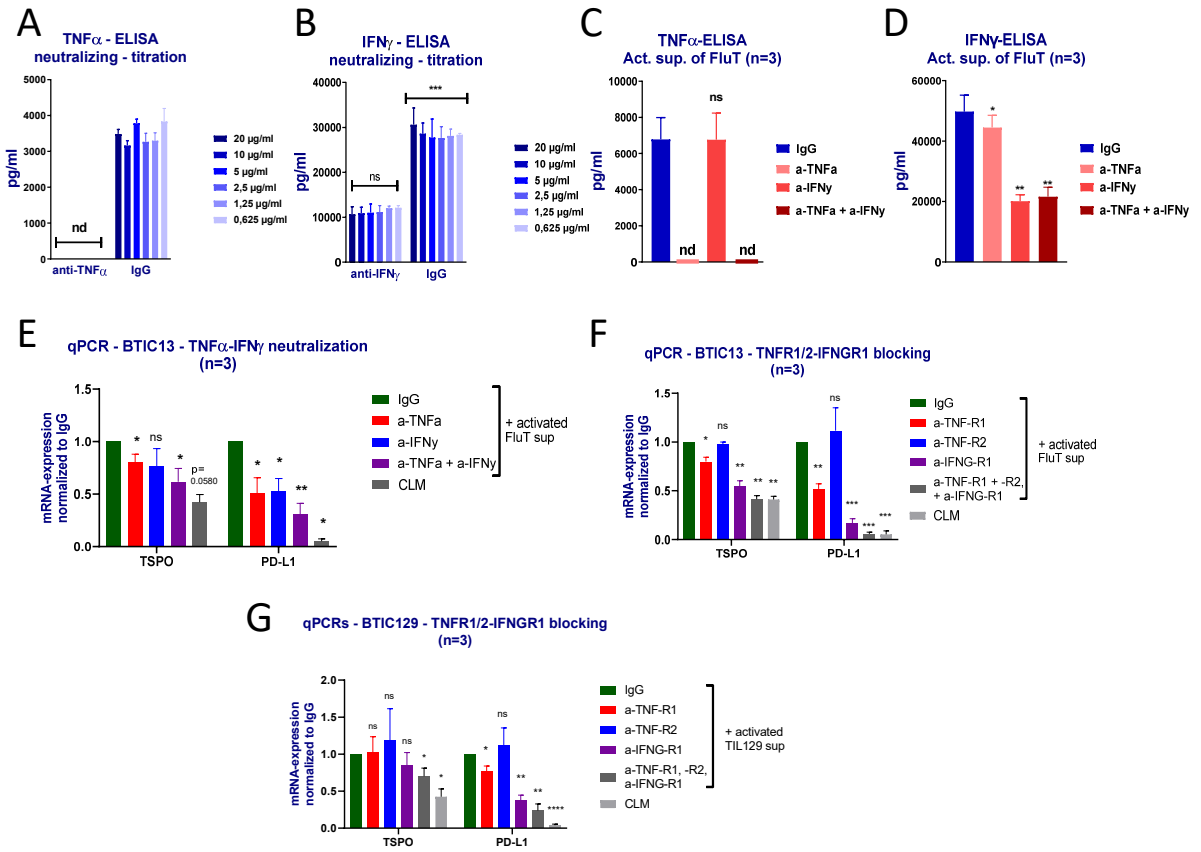

Figure 4: TSPO and PD-L1 expression of BTIC13 and BTIC129 after receptor blocking treatments. **(A-B)** ELISA for TNFα and IFNγ of supernatant containing antibodies against TNFα or IFNγ in concentrations ranging from 0,625 µg/mL to 20 µg/mL. **(C-D)** Compiled data from 3 independent ELISA experiments. Supernatants were previously treated with 2,5 µg/mL of a-TNFα antibody and/or 2,5 µg/mL of a-IFNγ antibody. **(A-D)** After 1h of incubation remaining cytokines were measured by in pg/mL, IgG was used as control. **(E)** Impact of cytokine-neutralized supernatant on TSPO and PD-L1 mRNA expression in BTIC13 **(F)** Impact of cytokine-receptor-blocking of BTIC13 and treatment with supernatant of FluT D11 cells on TSPO and PD-L1 mRNA expression **(G)** Impact of cytokine-receptor-blocking of BTIC129 and treatment with supernatant of TIL129 on TSPO and PD-L1 mRNA expression, **(E-G)** compiled out of three independent experiments. Values were normalized to IgG. Error bars indicate +/- SD. P-values were calculated using two-tailed paired student's t-test. * = $p < 0.05$, ** = $p < 0.01$, *** = $p < 0.005$, **** = $p < 0.001$.

3.5 TRAIL expression on FluT and TILs and its secretion after activation

Previously, my supervisor proved increased T cell- and TRAIL-mediated killing of primary glioblastoma cells if TSPO is downregulated. In these experiments TRAIL was used as additional treatment in kill assays. These findings and a part of the data discussed in this thesis were published in Acta Neuropathologica Communications (72). To determine the expression of TRAIL, FACS staining of non-activated, CD3-activated and CD3/CD28 (fully)-activated FluTC and TILs was performed (Figure 5A). Results show that the sole activation by CD3 increased the TRAIL expression compared to non-activated cells. Full activation resulted in an additional increase of TRAIL positive cells compared to CD3-activation. To quantify the amounts of soluble TRAIL secreted, supernatants of fully activated cells and of non-activated cells were analysed by ELISA. Results show that fully activated FluTC secreted with 9 pg/mL nearly 2,5 times more TRAIL than fully activated TILs with 4 pg/mL, while non-activated FluTC only show slight secretion of TRAIL (1,8 pg/mL) and non-activated TILs show none (Figure 5B).

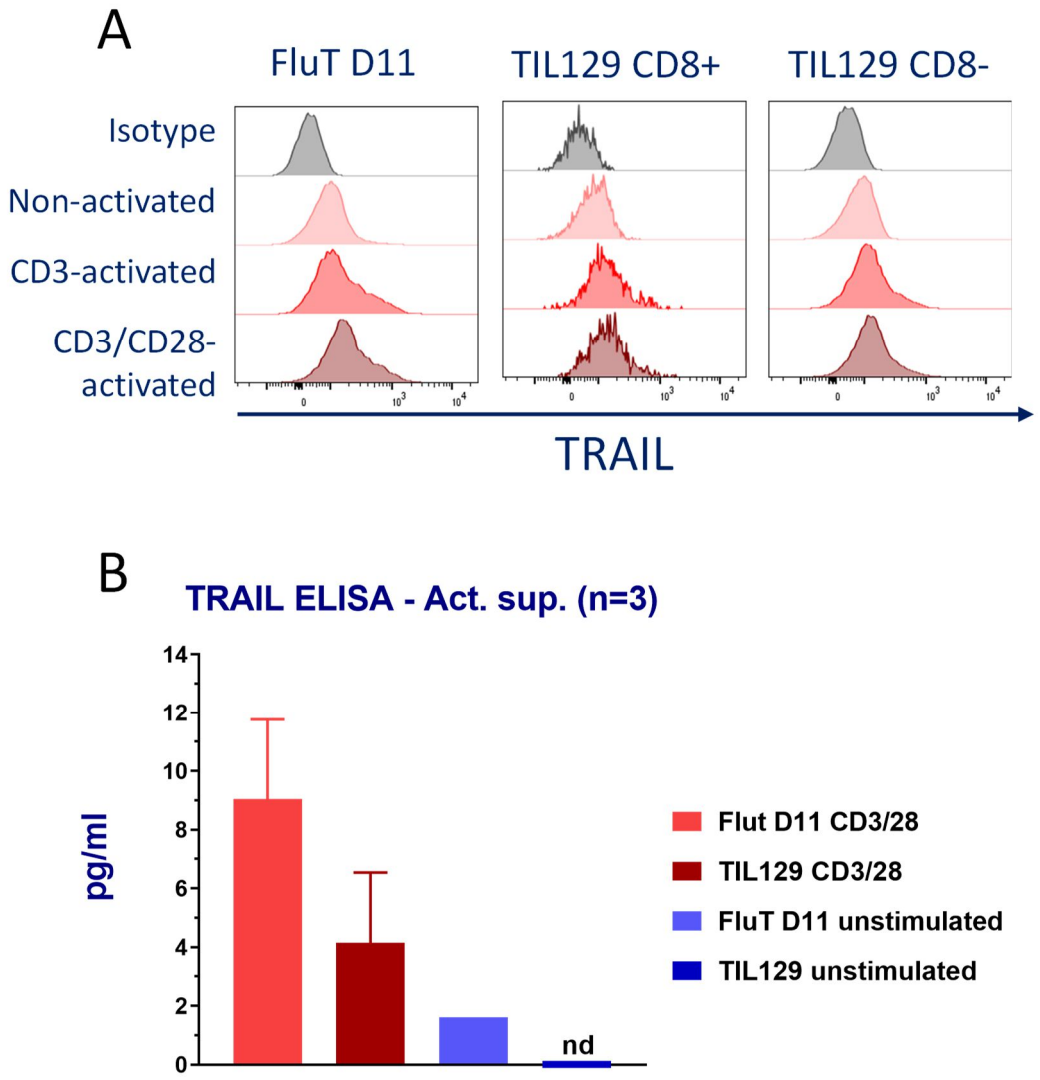

Figure 5: TRAIL expression on FluT D11 and on TIL129, TRAIL secretion of activated FluT D11 and TIL129. (A) TRAIL on FluT D11 and TIL129 was stained and analysed by FACS. Some cells were previously activated with CD3 and/or CD28. **(B)** Out of three experiments compiled ELISA of supernatants of CD3/CD28 activated FluT D11 and TIL129 and supernatants of non-activated FluT D11 and TIL129 cells. Secretion of cytokines in pg/mL. Error bars indicate +/- SD.

3.6 Characterization of U87 and U251 cells

As mentioned above, our group showed the tumor protective role of TSPO in primary glioblastoma cells. To validate this phenotype in classical glioblastoma cell lines, I reverse transfected U87 and U251 cells with TSPO-siRNA and co-cultured them with FluTC. First, the efficient ratio of FluT to glioblastoma cells had to be optimized. U87 and U251 cells were co-cultured with 2:1, 5:1 or 10:1 FluT to glioblastoma cells, and after 4h T cell mediated tumor cell killing was measured by XTT-Assay (Figure 6A). The ratio 10:1 killed 30% of U87 and 60% of U251 cells, 5:1 killed 20% of U87 and 25% of U251 and 2:1 killed less than 10% of U87 and almost no U251 cells. Knock-down efficiency of TSPO mRNA was measured by qPCR of TSPO-siRNA pool transfected U87 and U251 cells, compared to cells transfected with non-targeting-siRNA control Scr (scrambled sequence). Results exhibited 98% knockdown of TSPO mRNA in U87 and > 99% in U251 (Figure 6B). To find out how susceptible the expanded U87 and U251 cells are to FluTC and TRAIL/FasL interaction, they were FACS stained for Fas, DR4 and DR5. With circa 97% to 99%, both U87 and U251 cells presented an excessive expression of Fas. For TRAIL receptors DR4 and DR5 a divergent staining was observed. While DR5 is expressed by nearly all U87 and U251 cells, DR4 displays virtually no higher signal than control (Figures 6C-6D).

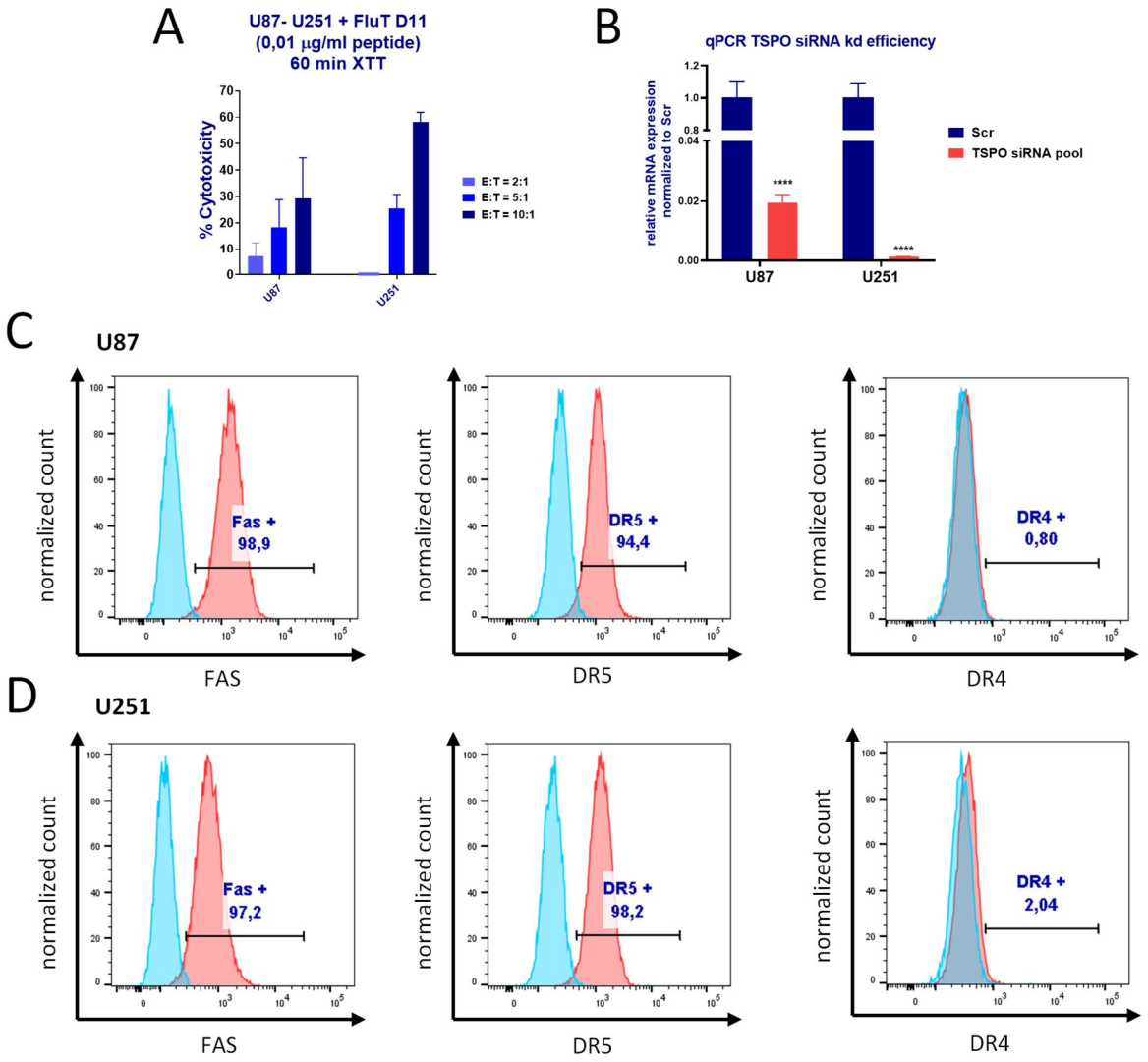

Figure 6: Characterization of U87 and U251 cells. (A) Cytotoxicity of U87 and U251 cells in %, tested with different ratios of effector cells (FluT) to target cells (U87 or U251), analysed via XTT-Assay. **(B)** Relative TSPO mRNA expression in TSPO-siRNA pool transfected U87 and U251 cells, compared to Scr (non-targeting control), compiled from two independent experiments. **(A-B)** Error bars indicate +/- SD. P-values were calculated using two-tailed paired student's t-test. * = $p < 0.05$, ** = $p < 0.01$, *** = $p < 0.005$, **** = $p < 0.001$. **(C-D)** FACS analysis of U87 and U251 cells, stained for Fas, DR4 and DR5. Isotype controls shown in blue, specific antibodies in red. Semi-logarithmic plot of receptor expression against normalized count of cells.

3.7 Impact of TSPO expression on T-cell mediated killing of U87 and U251 cells

For co-culture experiments, 5000 U87 or U251 cells were reverse transfected with either pool of four non overlapping siRNAs specific for TSPO mRNA or non-targeting control Scr4 for 72h. Afterwards, cells were pulsed 1h with Flu peptide. Then, either 20.000 or 40.000 FluTC were added and incubated for 4h. XTT-Assay was performed and cytotoxicity was measured. For U87, 60% for E:T ratio = 4:1 and 50% for E:T = 8:1 of the cells transfected with TSPO-siRNA were killed, while cells transfected with Scr4 as control were killed to either 30 % or 20 % (Figure 7A). For U251, 60% for E:T = 4:1 and 75 % for E:T = 8:1 of the cells transfected with TSPO-siRNA were killed, while cells transfected with Scr4 as control were killed to either 55% or 70%, respectively (Figure 7B). Next, I investigated whether downregulation of TSPO expression sensitizes glioblastoma cells to apoptosis. To this end, Caspase-3/7-Assays were performed where TSPO siRNA transfected U87 and U251 cells were treated with either FluTC or supernatant of activated FluTC (Figure 7C-7D). Results show that the treatment with FluTC and supernatant of activated FluTC activated Caspase-3/7 more when TSPO is downregulated: Transfected cells yielded circa 50% higher levels of active Caspase-3/7 for treatments with supernatant and for U87 cells, FluTC caused circa 50% more activation and for U251 cells only 15%, while the co-cultures with FluTC in general caused 10-fold (Figure 7C) and 40-fold (Figure 7D) higher values than treatment with supernatant. Co-culture of TSPO-deficient U87 cells with 50 ng/mL TRAIL (Figure 7E) yielded a slightly higher active Caspase-3/7 compared to TSPO-proficient cells, although the impact was not significant.

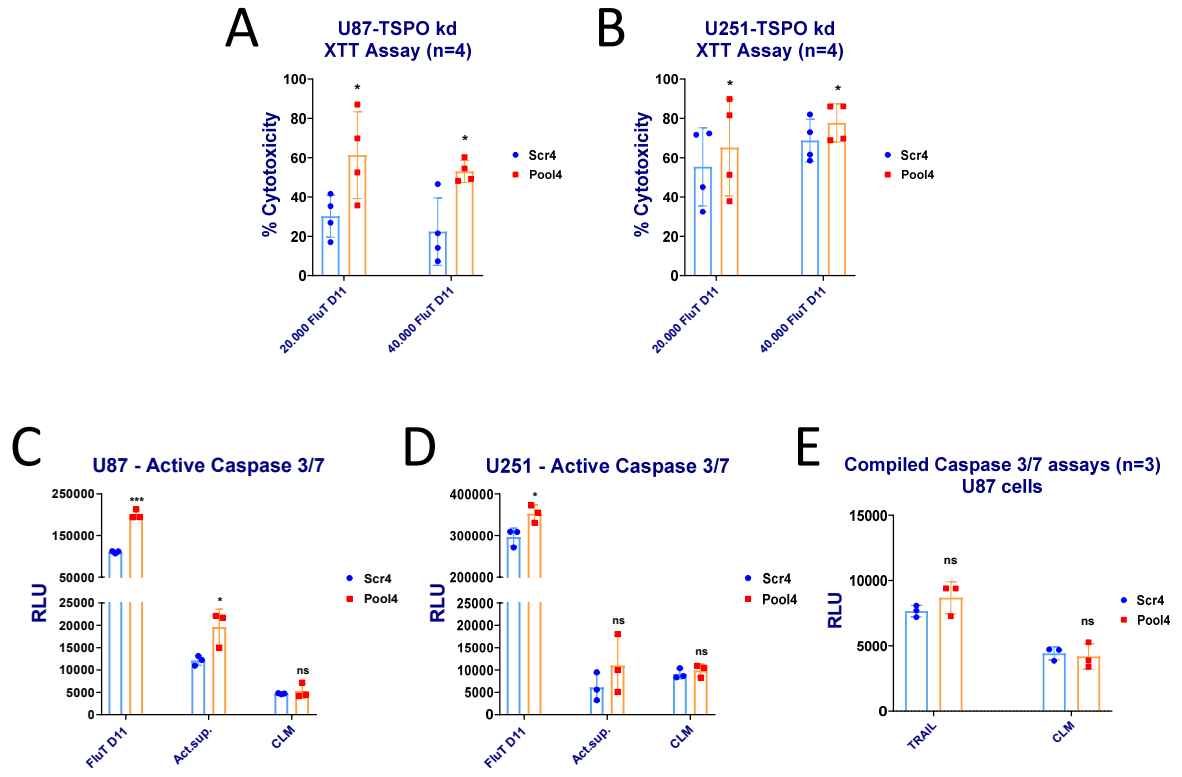

Figure 7: XTT- and Caspase-Assays of TSPO siRNA transfected U87 and U251 cells after treatments. **(A-B)** Compiled XTT-Assays of four experiments with 5000 TSPO siRNA transfected (Pool4) and control (Scr4) U87 and U251 cells. Cells were treated with 20.000 or 40.000 FluT D11 cells. Effect of the treatment was measured in percent of cytotoxicity. **(C-D)** Representative Caspase-Assays of TSPO siRNA transfected (Pool4) and control (Scr4) U87 and U251 cells. Cells were treated with 50.000 FluT D11 cells, supernatant of activated FluT D11 cells or CLM as control. Results measured in relative light units (RLU). (**E)** Compiled Caspase-Assays of 3 experiments with TSPO siRNA transfected (Pool4) and control (Scr4) U87 cells. Cells were treated with TRAIL or CLM, results were measured in RLU. All experiments were performed in triplicates, results for Caspase-Assays were read out after 30 minutes. Error bars indicate +/- SD. P-values were calculated using two-tailed paired student's t-test. * = $p < 0.05$, ** = $p < 0.01$, *** = $p < 0.005$, **** = $p < 0.001$.

4 Discussion

Even though immune therapies came a long way and drastically increased the survival of cancer patients in the last decades, glioblastoma still remains a malignant tumor with an unfavorable outcome. Immune checkpoint inhibition opened the path for new chances in treatment of cancers by preventing malignant cells to evade attacks by the immune system, yet there is still a high demand for better strategies to fight this entity of cancer.

In my thesis, I used FluTC and TILs to induce TSPO mRNA upregulation in primary glioblastoma cells. As GBM shows a distinct infiltration of T cells (20) and we hypothesized that TSPO can be upregulated in GBM in response to T cells and T cell-derived agents, I performed *in silico* analysis of correlation between *TSPO* mRNA and cytokine receptor mRNA expression in GBM to identify the cytokines that cause mRNA induction of TSPO (Fig. 1). Accordingly, I then first neutralized TNFα and IFNγ in the supernatant of activated FluTC and TILs. As the neutralization of IFNγ could not be achieved fully using neutralizing antibodies, TNF-R1, -R2 and IFNG-R1 were blocked on the cells themselves to hinder any possible signaling by the cytokines to the tumor cells. Here it became apparent that both cytokines play the main role in TSPO induction in BTIC13. Additionally, I focused on the impact of TSPO on the resistance against T cell- and TRAIL-mediated apoptosis of classical glioblastoma cell lines U87 and U251 and tested TRAIL as an inducer of apoptosis. For this I analysed the grade of TRAIL expression on FluTC and on TILs by FACS staining and the secreted amounts of TRAIL by these cells through ELISA. As the apoptosis of the tumor cells was induced by Fas and by TRAIL receptors DR4 and DR5, I examined the expression of these receptors on U87 and U251 by FACS analysis. Results show a higher cytotoxicity of U87 and U251 cells which were transfected with TSPO siRNA and treated with FluTC or supernatant, thus implying an anti-apoptotic role of TSPO in the tumor cells. Finally, the effect of TRAIL on transfected and non-transfected classical glioblastoma cell lines was determined by Caspase-3/7-Assays, indicating a tumor protecting role of TSPO against TRAIL-mediated apoptosis.

4.1 TNFα and IFNγ induce TSPO in primary glioblastoma cells

Initially, to investigate whether T cells can induce TSPO expression in glioblastoma cells, these were treated with FluTC, supernatant of activated FluTC and TILs and the changes of mRNA amounts of TSPO were measured by qPCR. Additionally, the concentrations of TNFα and IFNγ were determined by ELISA. For the analysis of BTIC13 and BTIC129 results show that the

induction of TSPO in FluTC + 0,001µg/mL of Flu peptide-treated tumor cells was nearly as high as in cells treated with supernatant of activated T cells. On the contrary, the concentrations of cytokines in the samples which were only treated with supernatant of activated FluTC are nearly 15 times higher than in the samples containing FluTC together with the highest concentration of Flu peptide. During the course of inflammation, as in GBM, brain tissue shows increased levels of TSPO (20). Therefore, these observations are based on the ability of FluTC, in contrast to the cell-free supernatant, to exert direct cytotoxic effects via the T-cell receptor. As the results for different concentrations of Flu peptide show, this protein is crucial for FluTC function (Fig. 2, Fig. 3A-3B). FluTC are cytotoxic T cells and act via secretion of granzymes and perforins, the Fas/FasL-axis (73), or other mechanisms like TRAIL-TRAIL-R-interaction (42). Earlier studies have shown that TSPO expression is mainly regulated through the PKC/ERK1/AP1/STAT3 signaling pathway (20). Concordantly, Fas activation also influences ERK1 (74), which might represent one reason for the TSPO induction, if concentrations of perforin, granzyme B and soluble Fas ligand in the supernatant of activated FluTC are low. The involvement of other mediators in the FluTC treated BTIC13 samples is pointed out further by the even lower concentration of TNFα and IFNγ in the co-culture with 0,0001 µg/mL, where even less cytokines were found while presenting a significant induction of TSPO.

The concentrations of TNFα and IFNγ secreted by FluTC are lower than those of FluTC supernatant due to the excessive activation of FluTC with CD3 and CD28 antibodies to generate the supernatant, whereas these antibodies were not added to the tumor cell-FluTC-Flu peptide co-culture. Accordingly, FluTC are not fully exhausted in terms of their cytokine-secreting activity by the specific tumor cell contact using Flu peptide. Significantly, the TSPO mRNA may only be upregulated to a certain point, so that even smaller amounts of cytokines may be sufficient for maximal mRNA expression.

For the experiment with BTIC129, additional supernatant of activated TILs of the same donor (TIL129) was used. Here the results are similar to those of the co-culture of BTIC13 and supernatant of activated FluTC, but the levels of TNFα and IFNγ in the supernatant of activated TIL129 are higher. This incidence may originate from the difference between TIL129 and FluTC. With the high immune resistance of GBM (75), TILs are pathologically less reactive against tumor cells through prolonged and repeated antigenic exposure (T cell exhaustion) (76). TILs would hardly induce TSPO through direct cytotoxic mechanisms because, as *in vivo*, contact with tumor cells is not sufficient to effectively target glioblastoma. However, after activation of TILs with CD3 and CD28 antibodies, they secrete TNFα and IFNγ even more than

FluTC. Accordingly, TILs retain their ability to secrete cytokines despite eventual T cell exhaustion. ELISA showed that FluTC secreted about five times more TRAIL than unstimulated cells following their antibody activation; activated TIL129 secreted 4 pg/mL, whereas TRAIL was undetectable in unstimulated TIL129. Flow cytometry was used to determine TRAIL expression on FluTC and TIL129 (Fig. 5), which was highest after CD3/CD28 activation but was already higher in unstimulated cells than in negative controls. Soluble TRAIL secreted by these cells presumably does not play a major role, since the supernatant of activated FluTC, at twice the TRAIL concentration, increased TSPO expression even less than the supernatant of activated TIL129 (Fig. 3). Also evident from Fig. 5A is that few of the TIL129 are CD8+, whereas almost all of the FluTC are CD8+ (Fig. 2B). Accordingly, the majority of TILs present in vivo are CD4+ cells, which classically serve as helper- instead of cytotoxic cells. However, this dichotomy is currently debated as CD4+ T cells demonstrated cytotoxic capabilities as well (77).

After demonstrating that TSPO can be induced by T cells and by their supernatant after CD3/CD28-activation, I aimed to investigate if the TSPO upregulation, that correlates with a higher malignancy (78) and worse prognosis for patients with GBM (20), is caused primarily by TNFα and IFNγ. For this, I first aimed to block both using anti-TNFα and anti-IFNγ antibodies. The concentration of the added antibodies was chosen after I tested the neutralizing effect by incubating CLM with artificially added cytokines with a range from 0,625 µg/mL to 20 µg/mL of neutralizing antibodies. ELISA results indicated full neutralization of TNFα even at the lowest concentration of neutralizing antibodies, while IFNγ was detected at every concentration of added antibodies at circa 40% of the basal level. Because the IFNγ amounts in every sample were reduced to the same level, insufficient concentrations of neutralizing antibody were unlikely the cause of this observation. Since remaining cytokines were to be measured from the co-culture supernatant in the experiment once more and TNFα was completely removed from the medium, I chose 2,5 µg/mL as concentration of neutralizing antibodies. qPCR results pointed out that TSPO and PD-L1 are less induced by BTIC13 when TNFα and IFNγ are neutralized, while the outcome of IFNγ-neutralization was not significant regarding TSPO expression (Fig. 4E).

Neutralizing TNFα caused a just slightly higher TSPO expression than neutralizing IFNγ, both neutralized reduced the expression to 60% of the basal upregulation when both cytokines were in original concentrations. The supernatant of this co-culture experiment yielded similar results as the ELISA used to find the right concentration of neutralizing antibodies. While the results

for TNFα in the co-cultures were not affected by this problem, IFNγ was only partially neutralized, therefore IFNγ interacted with the IFNG-R of the glioblastoma cells. Accordingly, TSPO and PD-L1 were upregulated by IFNγ in the respecting samples. To circumvent the problem of ineffective neutralization of IFNγ, receptors of the BTIC13 themselves were blocked by receptor blocking antibodies against TNF-R1, which is the main receptor for the known effects TNFα causes when interacting with cells, TNF-R2, not expected to be involved in carrying properties like TNF-R1 when interacting with TNFα, and IFNG-R1 as main receptor for IFNγ. The characteristics of TNF-R2 are not as well understood as those of TNF-R1, but it was reported that TNF-R2 propagates neuronal survival and TNF-R2-knockdown created a partial resistance against toxicity following injection of LPS, which would normally trigger a systemic inflammation (79). In epithelial ovarian cancer, TNF-R2 expression was associated with a poor prognosis (80). TNF-R2 expression therefore arguably correlates to cell survival and proliferative functionality.

The experiment was carried out in the same manner as the experiment with the neutralizing antibodies, while the blocking antibodies were added to the cells and incubated directly at a working concentration of 10 µg/mL for TNF-R1 and -R2 blocking antibodies. IFNG-R1 blocking antibodies were incubated at a concentration of 2 µg/mL. These concentrations were chosen to level above the concentrations of manufacturer's protocols to ensure a high effectivity of the antibodies. The outcome corresponded to the expectation that IFNγ was not fully neutralized in the experiment before, as the TSPO and PD-L1 inductions were lower in the samples where IFNG-R1 was blocked. Additionally, the samples with all receptors TNF-R1, -R2 and IFNG-R1 blocked showed the same level of upregulation of both TSPO and PD-L1 as the negative control CLM. This proved that TSPO induction in BTIC13 is caused mainly by TNFα and IFNγ. To generalize this phenomenon, the same experiment was performed with BTIC129 and this time supernatant of activated TILs from the same patient (TIL129). Here, qPCR presented less upregulation of TSPO and PD-L1 if the cells were protected from the exposure to TNFα, IFNγ or both, but not reaching the same low levels of the control suggesting that cytokine receptor interactions were not completely blocked in BTIC129 cells. This shows that the results of BTIC13 cannot be expected for every primary glioblastoma cell line. As BTIC13 and BTIC129 can already be set apart by morphology microscopically and by different behavior in cell culture, namely the better adhesional abilities of BTIC13 (mesenchymal subtype), their different reactions to the receptor blocking were anticipated. The highest expression of TSPO was described in the mesenchymal subtype, which showed the highest

level of immune cell infiltration compared to other subtypes. Contradictory, it was shown that the mesenchymal subtype shows the worst prognosis, even though a high immune infiltration in the brain may be seen as a better ability to respond to the tumor (20,81). I demonstrated that TNF-R1-blockade inhibits TSPO upregulation in mesenchymal GBM cells (BTIC13, Fig. 4F). In proneural cells (BTIC129, Fig. 4G), on the other hand, TSPO mRNA expression was not influenced. Cytokines like TNFα induce PN-MES switch (PMT) (82,83). This supports the role of TSPO in PMT: Assuming TSPO as progression marker, proneural cells would not be susceptible to TNFα induced PMT, while this mechanism is exerted in the already sensitized mesenchymal cells in situ. Differential observation of the presented subtype is important for prognosis as aggressive therapy of classical GBM has a greater effect than in proneural GBM (84).

Additionally, as a different supernatant was used for both experiments and in the latter both tumor and immune cells were donated from the same patient, it is likely that the abilities of the TILs are already restricted and that possibly other mediators were secreted by the TILs that induced the TSPO and PD-L1 upregulation even with effects of TNFα and IFNγ fully blocked. IFNγ is known to upregulate PD-L1 in GBM. Here, IFNγ conveys PD-L1 expression via JAK2/STAT1/IRF1-axis (25). IRF-1 (interferon regulatory factor 1) binds and activates the promoter of PD-L1, consequently increasing PD-L1 expression on GBM cells (38,85).

Once activated, TLRs induce inflammatory processes and PD-L1 gene transcription using the MyD88/TRAF6/MEK/ERK pathway (25,85). Regarding the immune response via TIL, an increase in PD-L1 in melanoma cells causes increased secretion of IFNγ and therefore inhibition of their own immune response (86) as chronic IFN exposure causes PD-L1 resistance (25).

Interestingly, the removal of TNFα also caused less upregulation of PD-L1 in the tumor cells. TNFα increases STAT3, a blockade of STAT3 might decrease immune resistance caused by PD-L1 (87,88). As described earlier, STAT3 is involved in TSPO upregulation (20), this provides an explanation for the property of TNFα to upregulate TSPO. TNFα expression itself is regulated by PD-L1 expression as CRISPR/Cas9 deletion of PD-L1 in U87 cells increased TNFα secretion by 2,5-fold (89). TNF-R activation increases TSPO also by ROS production through JNK-pathway (90). IFNG-R activation and TNFα production is mediated through ROS production (91), activated microglia and Th17 cells (33,92).

Microglia make up one third of the tumor mass in GBM (33) and TSPO is especially expressed by microglia, here predominantly by the M1 type, not by M2 (93). Further, TSPO inhibits M2 polarization in hypoxic brain ischemia (94). Contradictory, TSPO inhibits M1 polarization in cerebral-ischemia reperfusion injury (CIRI), opening the possibility for TSPO as a therapeutic target in patients with stroke (31). This shows the heterogeneity of TSPO in general and its variety depending on the current state of the cells.

GBM maintains its immune microenvironment utilizing TSPO: Yusuying et al. demonstrated upregulation of M2 marker TGFβ following injection of the TSPO ligand PK 11195, while TGFβ hindered transmigration of cytotoxic T cells and correlated with shorter survival (31,95). Interestingly, Song et al. described that TGFβ-mediated PMT in U87 was inhibited by the broadly used anti-diabetic metformin (96).

4.2 TSPO confers TRAIL-resistance in classical glioblastoma cells

The results of the experiments with primary glioblastoma cells demonstrate that TSPO is dynamically upregulated in cancer cells upon contact with T cells or their secreted cytokines. As studies described, TSPO is correlated to a more anti-apoptotic state of the cancer cells in classical GBM cell lines (20), therefore I used U87 and U251 to investigate the effect of TSPO on the ability to decrease apoptosis when exposed to FluTC and their supernatant after activation. Because classical cell lines are used most often in research and primary GBM behaves heterogeneous intertumorally, I wanted to investigate the role of TRAIL in context with TSPO, examining TRAIL as an interesting option to counter immune evasive mechanisms of tumor cells.

At first, I used FACS to determine the expression of membrane-bound TRAIL on FluTC and TIL in context with its state of activation by CD3 and or CD28. These antibodies mimic an in vivo situation where target cells express co-activating ligands, triggering a full immune response (97). Concordantly, TRAIL was upregulated highest after stimulation by both antibodies and, interestingly, in a similar fashion in both CD8 + and CD8 – TILs. Accordingly, soluble TRAIL was secreted to a higher extent as well once the immune cells were activated, while FluTC produced more TRAIL than TILs. This could be a sign for T cell exhaustion, as these cells are in contact with GBM cells and their immune suppressive environment.

FACS of U87 and U251 revealed a difference in TRAIL-R expression as that DR4 could not be detected in this experiment. Though GBM is a heterogenous tumor and therefore findings

on the distinctive function of DR4 and DR5 in anti-tumor activity are mixed, van Roosmalen et al. found that ectopic overexpression of DR5 in U87 cells would not enhance TRAIL sensitivity and TRAIL-induced apoptosis (98). While these cells were transduced by a lentiviral vector to increase DR5 expression, the cells I studied were not stimulated before FACS. This considered, these results pose a possible cause for the insignificant results of the Caspase-3/7-Assay with TRAIL-treated U87 cells (Fig. 7E), as TRAIL-induced apoptosis in U87 cells would mainly be conveyed via DR4 (98). Further, soluble TRAIL was proven to be more efficient when it is comprised in a membrane-bound conformation and murine TRAIL has a higher affinity to human TRAIL-R (42). We used plain recombinant human TRAIL, possibly reducing the effectiveness in our setup as well. Lower expression of TRAIL-R1 might promote immune evasion as R1 (DR4) is activated at lower, R2 (DR5) at higher concentrations of TRAIL (41).

Zeno et al. examined $CoCl_2$-induced apoptosis in U118 GBM cells and described that TSPO knockdown prevented apoptosis (99). General consensus confirms pro-apoptotic function of TSPO as well (20) and reportedly displays neuroprotective effects in Alzheimer's disease, Parkinson's disease and other brain injuries (58). However, in our results, TSPO is presented as anti-apoptotic when tumor cells are co-cultured with FluTC, or treated with activated T cell supernatant and TRAIL. Therefore, with the latter being expressed and secreted by the former, TSPO confers TRAIL resistance in GBM. Synthetic TSPO ligands with defined pharmacodynamics present a new approach in sensitizing GBM for TRAIL-mediated apoptosis.

Tumor cell-FluTC ratios of 4:1 and 8:1 were chosen for the transfection experiments to discover if cytotoxic effects depend on the quantity of FluTC. Apparently, the rate of the killed cells to FluTC counts behaves non-linear for the investigated ratios in U87, cytotoxicity and the effect of TSPO knockdown are similar, while overall cytotoxicity is pronounced in U251. As Figs. 7A and 7B show, TSPO knockdown ensures that both U87 and U251 are killed in higher numbers by FluTC. However, this effect is more pronounced in the U87 cell line. U87 are considered GBM cells of the neural subtype, while U251 are mesenchymal (100). Given the worse prognosis in patients with mesenchymal GBM (20) this finding substantiates TSPO as a possible prognostic marker.

Because TSPO ligands are not proven to act either agonistic or antagonistic, while partially agonistic behavior might also complicate interpretation of TSPO activation, I used the principle of RNA interference (RNAi) to knockdown TSPO mRNA in glioblastoma cells. Thereby TSPO reduction is objectifiable and off-target effects of TSPO ligands are ruled out (20,101). Here,

added siRNA enters into RISC (RNA induced silencing complex) and complementary pairs with its target mRNA. This causes a stop of further translation of the mRNA or otherwise initiates its degradation, acting as a defense mechanism against viruses through inhibition of replication. When siRNA binds unspecifically, it might cause off-target effects (102,103). It has been reported that miRNA, with similar function, is able to protect certain cell types from TRAIL-induced apoptosis. If siRNA (with analogue structure to human miRNA) is used in research or in therapy, interfering off-target effects could be prevented. For instance, miRNA-26a is highly expressed in TRAIL-resistant CLL cell lines and miRNA-145 is downregulated in colorectal and prostate cancer, both TRAIL-sensitive (104). MiRNA-133a contributes to TRAIL resistance in GBM by suppressing TRAIL-R2 expression (41). This shows that miRNA might be heavily involved in prevention of cancer cell apoptosis and therefore represents an intriguing therapeutic approach, but also indicates that siRNA transfection can distort outcomes due to undetected off-target effects.

Fas stimulation increases CAMK1D, which inhibits caspases 3 and 7 in anti-PD-L1 refractory tumors (105). Thus, the Caspase-3/7-Assay might not show the true state of apoptotic activity in the co-culture, as these enzymes are the final effectors in this setup. Differently than gliomas, GBM expresses a low level of caspase 8 (41). Caspase 8 is part of the early Caspase cascade, initially activated by FADD after Fas stimulation, it enhances mitochondrial cytochrome c release, and it cleaves Pro-caspases 3 and 7 to full activation (106,107). Hence, GBM generally exerts a natural resistance to caspase-induced apoptosis.

Lovastatin, a commonly applied HMG-CoA reductase inhibitor to decrease LDL blood levels, enhanced TRAIL-induced apoptosis in GBM. Considering the age of GBM patients and the broad use of this drug, some affected patients might already be profiting from this finding. Similar connections were discovered for valproic acid in GBM patients. This anticonvulsant, especially administered to adults, takes part in enhancement of TRAIL-induced apoptosis (1,41).

5 Conclusion and Outlook

Glioblastoma still represents one of the deadliest and most feared tumors. The often relatively young patients cannot expect a spectacular recovery like in the case of certain lymphomas. In this thesis I could show that TPSO expression can be upregulated in glioblastoma cells as a resistance mechanism if they encounter cytotoxic T cells or if they are treated with supernatant of activated cytotoxic T cells. The effect of cytokines TNFα and IFNγ, which are present in this supernatant, on TSPO expression has been demonstrated and it was shown that these cytokines play a substantial role in the upregulation of TSPO in glioblastoma cells. As the results of the experiment with the TSPO siRNA transfected classical glioblastoma cells have shown, TSPO expression in the cells reduced the ability of cytotoxic T cells to kill U87 and U251 cells. TSPO showed to have either pro-apoptotic or anti-apoptotic effects in the past, depending on the cell lines used in earlier studies. Here, TSPO knockdown unraveled pro-apoptotic effects in co-cultures with TRAIL, enabling the possibility of TSPO mediated TRAIL-resistance in GBM. With the emerging improvements in the design of specifically acting drugs through advanced techniques, TSPO ligands whose pharmacodynamics are precisely known could be developed. Thus, further investigation of the role of TSPO in T cell control and therapy resistance of GBM is necessary and promises a way to improve the prognosis of this so far incurable cancer.

6 Materials

6.1 Cell media and supplements

Material	Company
AIM V medium	Thermo Fisher Scientific
Dimethyl sulfoxide (DMSO)	Sigma-Aldrich
Fetal calf serum (FCS) (heat-inactivated)	Biochrom
IL-2 (human, recombinant)	Novartis
Penicillin/Streptomycin (P/S)	Sigma-Aldrich
DMEM-High Glucose (4.5 g/l), without sodium pyruvate	Sigma-Aldrich

6.2 Composition of cell media and buffers

Cell medium	Ingredients	Concentration	Volume
Coating Buffer (pH 9,5)	8,4 g NaHCO3 3,56 g Na2CO3 water		 1 L
Complete lymphocyte medium (CLM) for FluT cell (filtered after preparation)	RPMI AB serum HEPES P/S β-Mercaptoethanol	 10% 1% 1% 0,01 %	500 mL 50 mL 5 mL 5 mL 50 µL
FACS buffer	FCS PBS	2%	1 mL 50 mL
FluT expansion medium	CLM AIM-V	50 % 50 %	50 mL 50 mL
FluT expansion medium with feeder cells	CLM AIM-V	50 % 50 %	75 ml 75 ml

	Feeder cells OKT3 rHuIL-2	200x TILs 30 ng/mL 3000 U/mL	$200x10^6$ 4.5 µl 45 µl
Freezing medium A	FCS RPMI	60% 40%	21 mL 14 mL
Freezing medium B	FCS DMSO	80% 20%	28 mL 7 mL
RAV medium	RHB-A P/S EGF FGF2	 1% 50 ng/mL 50 ng/mL	50 mL 0,5 mL 10 µL 10 µL
Phosphate-buffered saline (PBS)	PBS 10x (Sigma-Aldrich) ddH2O		100 ml 900 ml
PBS-T (0,05%)	PBS Tween 20		1 L 500 µL

6.3 Chemicals and reagents

Material	**Company**
Assay Diluent	BD Bioscience
Accutase	Sigma-Aldrich
Benzonase (250 U/µL)	Merck
Beta-mercaptoethanol	Sigma-Aldrich
Bovine serum albumin (BSA)	Sigma-Aldrich
EDTA 1% (w/v) without Mg^{2+}	Biochrom
Ethanol absolute	Sigma-Aldrich
Flu peptide	Proimmune

IncuCyte® Caspase-3/7 Green Apoptosis Assay Reagent	Essen bioscience (Sartorius)
Kiovig	Baxter
Lipofectamine RNAiMAX	Thermo Fisher Scientific
Nuclease free water	Ambion
Phosphate saline buffer (PBS)	Sigma-Aldrich
Recombinant human IFNγ	PeproTech
Recombinant human TNFα	PeproTech
Trypan blue solution (0.4 %)	Fluka
Trypsin-EDTA (1x)	Lonza
Tween 20	Sigma-Aldrich
Zombie Aqua	BioLegend
Zombie NIR	BioLegend

6.4 Kits

Kit	**Company**
ELISA development kit for TNFα, IFNγ	BD Bioscience
ELISA development kit for TRAIL	R&D Systems
QuantiFast SYBR Green PCR Kit (qPCR)	Qiagen
QuantiTect Reverse Transcription Kit	Qiagen
RNeasy Mini Kit	Qiagen

6.5 Laboratory equipment

Machine	**Company**
BD FACS Lyric	BD Bioscience
FACSARIA II cell sorter	BD Bioscience

Luminex MAGPIX	Invitrogen
QuantStudio 3 Real-Time PCR System	Thermo Fisher Scientific
Spectrometer Scan Drop 250	Analytik Jena
TECAN SPARK 10M	TECAN

6.6 siRNAs

siRNA	Company
siRNA library – scr4	Horizon
TSPO siRNA library – pool4	Horizon

6.6 Primers

Primer	Sequence	Company
Human β-actin	F: CCT CGC CTT TGC CGA TCC R: GCG CGG CGA TAT CAT CAT CC	Merck
Human TSPO	F: TCT TTG GTG CCC GAC AAA T R: GGT ACC AGG CCA CGG TAG T	Merck
Human CD274 (PD-L1)	F: TGC CGA CTA CAA GCG AAT TAC TG R: CTG CTT GTC CAG ATG ACT TCG G	Merck

6.7 FACS antibodies

Specificity	Species	Isotype	Conjugate	Company	Dilution
Anti-human CD3	Mouse	IgG2a, κ	FITC	BioLegend	1:20
Anti-FAS	Mouse	IgG1, κ	BV421	BioLegend	1:20
Anti-human CD261 (DR4)	Mouse	IgG1, κ	APC	BioLegend	1:20
Anti-human CD262 (DR5)	Mouse	IgG1, κ	PE	BioLegend	1:20
Anti-human CD4	Mouse	IgG1, κ	PerCP-Cy5.5	BioLegend	1:100

Anti-human CD8	Mouse	IgG1, κ	V450	BD	1:100
Flu Pentamer (A*02:01 - GILGFVFTL, Influenza A MP 58-66)	-	-	APC	ProImmune	1:10
Isotype control	Mouse	IgG1	APC	eBioscience	1:20

6.8 Antibodies and recombinant proteins for functional assays

Antibody/Protein/Peptide	**Company**	**Working concentration**
Anti-human CD3 (clone: OKT3)	eBioscience	30 ng/ml for REP, 1 µg/mL for coating
Anti-human CD279 (PD-1)	BioLegend	0,5 µg/mL-20 µg/mL
Anti-human CD28	BioLegend	1 µg/mL
Anti-human IFNG-R1	R&D Systems	2 µg/mL
Anti-human IFNγ	R&D Systems	0,625 µg/mL-20 µg/mL
Anti-human TNF-R1	R&D Systems	10 µg/mL
Anti-human TNF-R2	R&D Systems	10 µg/mL
Anti-human TNFα	R&D Systems	0,625 µg/mL-20 µg/mL
IgG1 Protein, human, recombinant (103 Cys/Ser)	Sino Biological	200 nM
Matched peptide A*02:01-GILGFVFTL	ProImmune	0,01 µg/mL

6.9 Consumables

Material	**Company**
Cryogenic vials (2 mL)	Corning
Conical centrifuge tubes (15 mL and 50 mL)	TPP
FACS tubes	Falcon

Flat bottom plates (6 and 96 wells)	TPP
NUNC MaxiSorp 96 wells ELISA plates	Thermo Fisher Scientific
PCR micro test tube	Nerbe plus
Pipette filter tips (10 µL - 1000 µL)	Thermo Fisher Scientific
Polysorp 96 well plates	Thermo Fisher Scientific
Polystyrene round bottom tubes with caps	Falcon
Reservoir 10-25 mL sterile	INTEGRA Biosciences
Round-bottom plate (96 wells)	TPP
Safe-lock tubes (0.5 mL, 1.5 mL, 2.0 mL)	Eppendorf
Tissue culture flask/filter cap (25 cm^2, 75 cm^2, 150 cm^2)	TPP
Tissue Culture Treated Plate (6, 24 wells)	Merck
U-bottom plate (96 wells)	TPP
Ultrafree-MC centrifugal filter	Merck
V-bottom plate (96 wells)	Greiner Bio-One

6.10 Software

Software	**Company**
FlowJo	FlowJo
GraphPad Prism 8	GraphPad Software
Microsoft Office 2019	Microsoft

7 Methods

7.1 Cell culture

7.1.1 BTICs (Brain tumor initiating cells)

BTICs are human primary glioblastoma cells that are generated from glioblastoma tissues obtained from patients and were kindly provided by the department of Neurooncology of UKR. The cells were cultured in cell culture flasks with BTIC medium, consisting of RHB-A medium with 1% P/S, 20 ng/mL EGF and 20 ng/mL FGF2. Cells were washed with PBS and detached by adding 5 mL of accutase and split in various ratios once they reached more than 70% confluency. The cells were frozen by resuspending them in 90% BTIC medium and 10% dropwise added DMSO. Afterwards the cells were cooled down 1 °C per minute in -80 °C using freezing containers and stored in liquid nitrogen.

7.1.2 U87 and U251 cells

Glioblastoma cell lines U87 and U251 were cultured in high glucose DMEM supplemented with 10 % FCS and 1 % P/S. Cells were washed with PBS and detached by adding 5 mL of trypsin and split in various ratios when they reached more than 70 % confluency. The cells were frozen by first resuspending them in freezing medium A (40 % RPMI, 60 % FCS) and then adding dropwise freezing medium B (20 % DMSO, 80 % FCS) in a 1:1 ratio. Finally, the cells were cooled down 1 °C per minute in -80 °C using freezing containers and were afterwards stored in liquid nitrogen.

7.1.3 FluT cells and TILs

Frozen FluTC and tumor-infiltrating lymphocytes (TILs) were thawed and added dropwise to 10 mL of complete lymphocyte medium (CLM) containing 50 IU/mL of benzonase. DMSO was removed by centrifugation and the cell pellet was resuspended in 1 mL of CLM per $1x10^6$ cells. The FluTC and TILs were incubated for at least 4h at 37 °C, 5 % CO_2 before performing experiments.

7.2 Generation and expansion of FluT cells

For the generation of Flu-specific CD8+ T cells, CD8+ T cells were isolated by my supervisor from peripheral blood mononuclear cells (PBMCs) of an HLA-A2 positive healthy donor and then antigen-specifically expanded while being exposed to A2-matched Flu peptide in the presence of low dose IL-2 and IL-15. To specifically expand the Flu-specific T cells, cells

obtained from antigen-specific expansion were stained with Flu-Pentamer and sorted using FACS. After sorting, FluTC were further expanded according to the rapid expansion protocol. To this end PBMCs from three different healthy donors were irradiated with 60 Gy and used as feeder cells. $1x10^6$ sorted FluTC and irradiated feeder cells were mixed in a 1:200 ratio and cultured in 150 mL of expansion medium supplemented with 30 ng/mL anti-CD3-AB (clone OKT3) and 3000 IU/mL IL-2 in a T175 flask. Cells were incubated for five days. Afterwards, 100 mL of medium was extracted while avoiding to stir cells up. This extract was centrifuged, the pellet was resuspended with 100 mL of fresh expansion medium and added back to the flask together with 3000 IU/mL of IL-2. On day 7 and 11 of expansion, medium was exchanged in the same manner as on day 5. Cells were counted and split to keep the cells at a concentration of $6x10^5$ cells/mL. On day 14, Flu-pentamer staining of 300.000 cells was done to check the percentage of CD8+ FluTC with FACS. The rest of the cells were frozen in aliquots of $5x10^6$ and $10x10^6$ cells by first resuspending them in freezing medium A (40% RPMI, 60% FCS) and then adding dropwise freezing medium B (20% DMSO, 80% FCS) in a 1:1 ratio.

7.3 Molecular biology techniques

7.3.1 RNA-Isolation and reverse transcription

To isolate RNA, cells were centrifuged for 10 min at 500 g and 4 °C. The cell pellet was washed once with 1 mL PBS and stored at -80 °C. The RNA was isolated using the Qiagen RNeasy Mini Kit according to the protocol of the manufacturer and was eluted with 30 µL of nuclease free water. The RNA concentration was measured using the Scan Drop (AnalytikJena). 1 µg RNA in 12 µL water was reverse transcribed into cDNA using the QuantiTect Reverse Transcription Kit. At first, 2 µL gDNAse (7x) were added to the samples. After incubation in the SimpliAmp thermal cycler for 3 min at 42 °C, 6 µL of a master mix containing 4 µL buffer, 1 µL random hexamer primer and 1 µL reverse transcriptase were added. The RNA samples were incubated for 20 min at 42 °C and the reverse transcriptase was heat-inactivated for 3 min at 95 °C. The cDNA was stored at -20 °C.

7.3.2 Real-time quantitative PCR

Real-time quantitative PCR (qPCR) was performed by adding 2 µL of 1:10 diluted cDNA (5 ng/µL) to 18 µL of a master mix containing 10 µL 2x QuantiFast SYBR Green PCR mix, 1,2 µL forward and reverse Primer (5 µmol/L) for the respective genes of interest and 5,6 µL nuclease-free water. Each sample was prepared in triplicates. The qPCR reactions were run

using the QuantStudio 3 (Applied Biosystems). The expression of β-actin was used for normalization and relative quantification was performed using the delta-delta Ct method.

7.3.3 Reverse siRNA transfection

To knock-down TSPO mRNA in U87 and U251 cells, siRNA transfection was performed. 200 µL of 250 nmol/L of siRNA solution were added per 6-well. RNAiMAX was diluted 1:50 with RPMI medium and incubated for 10 min at RT. 400 µL of RPMI per well were added and 600 µl of RNAiMAX-RPMI mix was pipetted on top of the siRNA and incubated for 30 min at RT. After incubation, $2x10^5$ U87 and U251 cells were resuspended in 1,2 mL of DMEM supplemented with 10 % FCS and seeded into the siRNA-RNAiMAX containing wells and incubated for 72 h at 37 °C. For reverse transfection in 96-well plates, this protocol was proportionally reduced adjusting the added amount of siRNA to 10 µL instead of 200 µL. 200.000 and 5.000 U87 and U251 cells were seeded per 6- and 96-well respectively.

7.4 Immunological techniques

7.4.1 Flu-Pentamer staining of FluTC

FACS staining with Flu-pentamer was performed to determine the percentage of Flu-specific CD8 positive T cells in a population. The Flu-pentamer consists of five MHC I Flu-peptide complexes conjugated with APC. $3x10^5$ FluTC were transferred to FACS tubes. The cells were washed with 1 mL FACS buffer and blocked with 100 µL Kiovig, diluted 1:20 in FACS buffer for 20 min on ice to reduce unspecific antibody binding. After blocking, cells were washed with cold FACS buffer and then live/dead staining was performed using Zombie Aqua dye (diluted 1:1000 in 100 µL PBS). After 15 min in the dark at RT, cells were washed with FACS buffer and stained with 50 µL Flu-pentamer, earlier centrifuged at 14.000 g for 5 min at 4 °C diluted 1:10 in FACS buffer for 10 min at RT in the dark. After washing, cells were stained with 50 µL anti-CD8-V450, diluted 1:10 in FACS buffer, for 20 min on ice in the dark. Hereafter, cells were washed, resuspended in 250 µL FACS buffer and acquired with the FACS Lyric machine. FlowJo software was used to analyse the FACS data.

7.4.2 Surface staining for TRAIL receptors on FluTC and TILs

To measure the impact of CD3 and CD3/CD28 activation of FluTC and TILs on the TRAIL expression, FACS staining was performed. FluTC were transferred to FACS tubes, were washed with 1 mL FACS buffer and blocked with 150 µL Kiovig, diluted 1:20 in FACS buffer for 20 min on ice to reduce unspecific antibody binding. After blocking, cells were washed with

cold FACS buffer and then live/dead staining was performed using Zombie NIR (diluted 1:1000 in 100 µL PBS). After 15 min in the dark at RT, cells were washed with FACS buffer and stained with anti-CD3-FITC, anti-CD4-PerCp-Cy5.5., anti-CD8-V450 and anti-human CD253-APC for 30 min on ice in the dark. Then, cells were washed, resuspended in 250 µL FACS buffer and acquired with the FACS Lyric machine. FlowJo software was used to analyse the FACS data.

7.4.3 Surface staining for FAS, DR4 and DR5 receptors on U87 and U251 cells

10^5 U87 and U251 cells were transferred to FACS tubes. The cells were washed with 1 mL FACS buffer and blocked with 100 µL Kiovig, diluted 1:20 in FACS buffer for 20 min on ice to reduce unspecific antibody binding. After blocking, cells were washed with cold FACS buffer and then live/dead staining was performed using Zombie NIR (diluted 1:1000 in 100 µL PBS). After 15 min in the dark at RT, cells were washed with FACS buffer and stained with anti-FAS-BV421, anti-human CD261-APC and anti-human CD262-PE for 20 min on ice in the dark. Then, cells were washed, resuspended in 250 µL FACS buffer and acquired with the FACS Lyric machine. FlowJo software was used to analyse the FACS data.

7.4.4 Generation of supernatant of activated T cells

Untreated 6-well plates were coated with 2 mL PBS per well, containing 4 µg/mL anti-CD3 antibodies (clone OKT3) and incubated at 4 °C overnight. The next day, unbound anti-CD3 solution was removed and the wells were washed with PBS before seeding $1x10^6$ FluT/mL in 5 mL CLM per well. Anti-CD28 antibodies were added at a final concentration of 1 µg/mL to the respective wells. Then, the T cells were incubated for 24h at 37 °C, 5 % CO_2. After incubation, cells were centrifuged at 1400 rpm at 20 °C for 10 min and cell free supernatant was collected and stored at -20 °C.

7.4.5 Experiments with anti-TNFα- and anti-IFNγ-neutralizing antibodies

In treated 6-well TPP plates 400.000 BTIC13 were seeded in 2 mL BTIC medium (see Materials) per well. On the next day, cell medium was removed and cells were treated with 1,5 mL of supernatants of activated FluT D11 cells. Prior to treatment, supernatants were incubated for 2h with either 5 µg/mL IgG, 2,5 µg/mL anti-human-TNFα-AB, 2,5 µg/mL anti-human-IFNγ-AB, or 2,5 µg/mL anti-human-TNFα-AB together with 2,5 µg/mL anti-human-IFNγ-AB. IgG was added to the samples to even the concentration of added AB to 5 µg/mL. CLM was used to measure the basal level of TSPO and PD-L1 expression. After 24h of incubation of tumor cells with antibody treated supernatant or CLM, cell medium was removed and wells

were washed with 2 mL PBS. Then, 500 µL of accutase per well were added and incubated for 3 min to detach the cells. 1 mL cold PBS was added in each well and cells were collected and stored at -80 °C.

7.4.6 Experiments with TNF-R1-, -R2- and IFNG-R1-blocking antibodies

400.000 BTIC13 or BTIC129 were seeded in 2 mL BTIC medium (see Materials) per well one day prior to treatment. If BTIC129 were used, treated 6-well TPP plates were coated with 500 µL of 10 µg/mL laminine, diluted in PBS. Cells were incubated at 37 °C, 5 % CO_2 for 2h. After incubation, cell medium was removed and 500 µL CLM were added per well. Either IgG, anti-human-TNF-R1-AB, anti-CD26, anti-human-TNF-R2-AB, anti-human-IFNG-R1-AB or all three together were added to the cells and incubated for 1h. Next, 1,5 mL of supernatant of activated FluT D11 cells for BTIC13 and supernatant of activated TIL129 for BTIC129 were added, resulting in 2 mL total medium per well, with concentrations of 10 µg/mL for both anti-TNF-R1-AB and anti-TNF-R2-AB and 2 µg/mL for anti-IFNG-R1-AB. IgG was added to keep the concentration of added ABs in total at 22 µg/mL. CLM was used to measure the basal level of TSPO and PD-L1 expression. After 24h of incubation, cell medium was removed and wells were washed with 2 mL PBS. Then, 500 µL accutase per well were added and incubated for 3 min to detach the cells. 1 mL cold PBS was added in each well and cells were collected and stored at -80 °C.

7.4.7 TNFα- and IFNγ - ELISA

To measure the concentration of TNFα and IFNγ in the supernatant of co-cultures, NUNC MaxiSorp 96-well ELISA plates were coated one day earlier with 100 µL per well coating solution, consisting of the respective capture antibody diluted 1:250 in coating buffer and incubated at least 12h at 4 °C. The coated ELISA plates were washed twice with 0,05 % PBS-T and blocked for 1h at RT in the dark with 100 µL assay diluent per well. After blocking, the plates were washed three times with PBS-T and 100 µL of standards or samples were added to each well. The 96-well plates were incubated for 2h at RT in the dark and were then washed five times with PBS-T. Afterwards, 100 µL of biotinylated detection antibody with Streptavidin-HRP diluted 1:250 in assay diluent were added per well and the plate was incubated for 1h at RT in the dark. After washing the plates seven times with PBS-T, 100 µL of substrate reagent, consisting of solution A and B in a 1:1 ratio, were added and the plates were incubated until the standards turned blue. To stop the reaction, 50 µL of 2 *N* H_2SO_4 were pipetted on top of the solution. At the end, the absorbance was measured at 450 nm with the TECAN reader using 570 nm as reference wavelength.

7.4.8 TRAIL - ELISA

NUNC MaxiSorp 96-well ELISA plates were coated one day earlier with 100 µL per well coating solution, consisting of the respective capture antibody diluted 1:120 in coating buffer and incubated at least 12h at 4 °C. The coated ELISA plates were washed three times with 0,05% PBS-T and blocked for 1h at RT in the dark with 300 µL assay diluent per well. After blocking, the plates were washed three times with PBS-T and 100 µL of standards ranging from 0 to 1500 pg/mL or 100 µL undiluted supernatant were added to each well. The 96-well plates were incubated for 2h at RT in the dark and were then washed three times with PBS-T. Afterwards, 100 µL of detection antibody diluted 1:60 in assay diluent containing 2% heat inactivated normal goat serum were added per well and the plate was incubated for 2h at RT in the dark. After washing the plates three times with PBS-T, 100 µL of 1:40 diluted Streptavidin-HRP solution were added to the wells and incubated for 20 min in the dark. Then, the wells were washed again three times and 100 µL of substrate solution, consisting of solution A and B in a 1:1 ratio, were added and the plates were again incubated in the dark for 20 min. At last, 50 µL of stop solution, 2 *N* H_2SO_4 were added from the top. Then the absorbance was measured at 450 nm with the TECAN reader using 570 nm as reference wavelength.

7.4.9 XTT-Assay

96-well plates with reverse siRNA transfected and variously treated U87 and U251 cells were analysed. PMS (phenazine methosulfate) was diluted 1:50 in XTT-reagent. 50 µL of this dilution were added per well and then analysed by TECAN reader at 450 nm using a reference wavelength of 650 nm. The cytotoxicity and viability of the cells were calculated as followed:

$$\text{viability [\%]} = [(OD_{E+T} - OD_E) / (OD_T - OD_{Med})] \times 100$$

$$\text{cytotoxicity [\%]} = 100 - \text{viability [\%]}$$

Where ‘E’ means the optical density (OD) of the sample containing effector cells only, ‘T’ means the OD of the sample containing only the target cells and ‘Med’ means the OD of the respective medium, in which the cells were added.

7.4.10 Luciferase-based Caspase-3/7 Assay

96-well plates with reverse siRNA transfected U87 and U251 cells were analysed after treatment with either 50.000 FluT D11 cells, supernatant of activated FluT D11 cells or CLM. Content of one bottle Caspase-Glo ® 3/7 (Promega) buffer was added to one bottle of lyophilized Caspase-Glo ® 3/7 substrate and mixed well. 100 µL of this solution were added per well. Plates were incubated in the dark at RT for 30 min on a plate shaker at 500 rpm and then analysed by TECAN reader at 450 nm using a reference wavelength of 650 nm.

7.5 Statistical evaluation

For the statistical evaluation GraphPad Prism 8 software was used. Statistical differences between the control and the test groups were determined using a two-tailed unpaired or paired student's t-test. T-tests with p-value < 0.05 were taken as significant and the levels of statistical significance were set as * = $p < 0.05$, ** = $p < 0.01$, *** = $p < 0.005$, **** = $p < 0.001$.

8 References

1. Weller M, Wick W, Aldape K, Brada M, Berger M, Pfister SM, Nishikawa R, Rosenthal M, Wen PY, Stupp R, Reifenberger G. Glioma. Nat Rev Dis Primers. 2015;115017. doi:10.1038/nrdp.2015.17 Cited in: PubMed; PMID 27188790.
2. Persaud-Sharma D, Burns J, Trangle J, Moulik S. Disparities in Brain Cancer in the United States: A Literature Review of Gliomas. Med Sci (Basel). 2017;5(3). doi:10.3390/medsci5030016 Cited in: PubMed; PMID 29099032.
3. Wirsching H-G, Galanis E, Weller M. Glioblastoma. Handb Clin Neurol. 2016;134381–97. doi:10.1016/B978-0-12-802997-8.00023-2 Cited in: PubMed; PMID 26948367.
4. Alifieris C, Trafalis DT. Glioblastoma multiforme: Pathogenesis and treatment. Pharmacol Ther. 2015;15263–82. doi:10.1016/j.pharmthera.2015.05.005 Cited in: PubMed; PMID 25944528.
5. McFaline-Figueroa JR, Wen PY. The Viral Connection to Glioblastoma. Curr Infect Dis Rep. 2017;19(2):5. doi:10.1007/s11908-017-0563-z Cited in: PubMed; PMID 28233187.
6. Chi J, Gu B, Zhang C, Peng G, Zhou F, Chen Y, Zhang G, Guo Y, Guo D, Qin J, Wang J, Li L, Wang F, Liu G, Xie F, Feng D, Zhou H, Huang X, Lu S, Liu Y, Hu W, Yao K. Human herpesvirus 6 latent infection in patients with glioma. J Infect Dis. 2012;206(9):1394–8. doi:10.1093/infdis/jis513 Cited in: PubMed; PMID 22962688.
7. Hardell L, Carlberg M. Mobile phones, cordless phones and the risk for brain tumours. Int J Oncol. 2009;35(1):5–17. doi:10.3892/ijo_00000307 Cited in: PubMed; PMID 19513546.
8. Kanu OO, Hughes B, Di C, Lin N, Fu J, Bigner DD, Yan H, Adamson C. Glioblastoma Multiforme Oncogenomics and Signaling Pathways. Clin Med Oncol. 2009;339–52. doi:10.4137/cmo.s1008 Cited in: PubMed; PMID 19777070.
9. Maher EA, Brennan C, Wen PY, Durso L, Ligon KL, Richardson A, Khatry D, Feng B, Sinha R, Louis DN, Quackenbush J, Black PM, Chin L, DePinho RA. Marked genomic differences characterize primary and secondary glioblastoma subtypes and identify two distinct molecular and clinical secondary glioblastoma entities. Cancer Res. 2006;66(23):11502–13. doi:10.1158/0008-5472.CAN-06-2072 Cited in: PubMed; PMID 17114236.
10. Martins TA, Schmassmann P, Shekarian T, Boulay J-L, Ritz M-F, Zanganeh S, vom Berg J, Hutter G. Microglia-Centered Combinatorial Strategies Against Glioblastoma. Front

Immunol. 2020;11571951. doi:10.3389/fimmu.2020.571951 Cited in: PubMed; PMID 33117364.

11. Miyake M, Tanaka N, Asakawa I, Yamaki K, Inoue T, Suzuki S, Hori S, Nakai Y, Anai S, Torimoto K, Toritsuka M, Nakagawa H, Tsukamoto S, Fujii T, Ohbayashi C, Hasegawa M, Kasahara M, Fujimoto K. A prospective study of oral 5-aminolevulinic acid to prevent adverse events in patients with localized prostate cancer undergoing low-dose-rate brachytherapy: Protocol of the AMBER study. Contemp Clin Trials Commun. 2020;19100593. doi:10.1016/j.conctc.2020.100593 Cited in: PubMed; PMID 32637724.

12. Nduom EK, Wei J, Yaghi NK, Huang N, Kong L-Y, Gabrusiewicz K, Ling X, Zhou S, Ivan C, Chen JQ, Burks JK, Fuller GN, Calin GA, Conrad CA, Creasy C, Ritthipichai K, Radvanyi L, Heimberger AB. PD-L1 expression and prognostic impact in glioblastoma. Neuro Oncol. 2016;18(2):195–205. doi:10.1093/neuonc/nov172 Cited in: PubMed; PMID 26323609.

13. Stupp Roger, Mason Warren P., van den Bent Martin J., Weller Michael, Fisher Barbara, Taphoorn Martin J.B., Belanger Karl, Brandes Alba A., Marosi Christine, Bogdahn Ulrich, Curschmann Jürgen, Janzer Robert C., Ludwin Samuel K., Gorlia Thierry, Allgeier Anouk, Lacombe Denis, Cairncross J. Gregory, Eisenhauer Elizabeth, Mirimanoff René O. Radiotherapy plus Concomitant and Adjuvant Temozolomide for Glioblastoma.

14. Davis ME. Glioblastoma: Overview of Disease and Treatment. Clin J Oncol Nurs. 2016;20(5 Suppl):S2-8. doi:10.1188/16.CJON.S1.2-8 Cited in: PubMed; PMID 27668386.

15. Huang B, Li X, Li Y, Zhang J, Zong Z, Zhang H. Current Immunotherapies for Glioblastoma Multiforme. Front Immunol. 2020;11603911. doi:10.3389/fimmu.2020.603911 Cited in: PubMed; PMID 33767690.

16. Hanif F, Muzaffar K, Perveen K, Malhi SM, Simjee SU. Glioblastoma Multiforme: A Review of its Epidemiology and Pathogenesis through Clinical Presentation and Treatment. Asian Pac J Cancer Prev. 2017;18(1):3–9. doi:10.22034/APJCP.2017.18.1.3 Cited in: PubMed; PMID 28239999.

17. Werry EL, Barron ML, Kassiou M. TSPO as a target for glioblastoma therapeutics. Biochem Soc Trans. 2015;43(4):531–6. doi:10.1042/BST20150015 Cited in: PubMed; PMID 26551689.

18. Holland EC. Glioblastoma multiforme: the terminator. Proc Natl Acad Sci U S A. 2000;97(12):6242–4. doi:10.1073/pnas.97.12.6242 Cited in: PubMed; PMID 10841526.

19. Behnan J, Finocchiaro G, Hanna G. The landscape of the mesenchymal signature in brain tumours. Brain. 2019;142(4):847–66. doi:10.1093/brain/awz044 Cited in: PubMed; PMID 30946477.

20. Ammer L-M, Vollmann-Zwerenz A, Ruf V, Wetzel CH, Riemenschneider MJ, Albert NL, Beckhove P, Hau P. The Role of Translocator Protein TSPO in Hallmarks of Glioblastoma. Cancers (Basel). 2020;12(10). doi:10.3390/cancers12102973 Cited in: PubMed; PMID 33066460.

21. El Atat O, Naser R, Abdelkhalek M, Habib RA, El Sibai M. Molecular targeted therapy: A new avenue in glioblastoma treatment. Oncol Lett. 2023;25(2):46. doi:10.3892/ol.2022.13632 Cited in: PubMed; PMID 36644133.

22. Lamouille S, Xu J, Derynck R. Molecular mechanisms of epithelial-mesenchymal transition. Nat Rev Mol Cell Biol. 2014;15(3):178–96. doi:10.1038/nrm3758 Cited in: PubMed; PMID 24556840.

23. Watanabe T, Hirota Y, Arakawa Y, Fujisawa H, Tachibana O, Hasegawa M, Yamashita J, Hayashi Y. Frequent LOH at chromosome 12q22-23 and Apaf-1 inactivation in glioblastoma. Brain Pathol. 2003;13(4):431–9. doi:10.1111/j.1750-3639.2003.tb00474.x Cited in: PubMed; PMID 14655749.

24. Mitsuka K, Kawataki T, Satoh E, Asahara T, Horikoshi T, Kinouchi H. Expression of indoleamine 2,3-dioxygenase and correlation with pathological malignancy in gliomas. Neurosurgery. 2013;72(6):1031-8; discussion 1038-9. doi:10.1227/NEU.0b013e31828cf945 Cited in: PubMed; PMID 23426156.

25. Litak J, Mazurek M, Grochowski C, Kamieniak P, Roliński J. PD-L1/PD-1 Axis in Glioblastoma Multiforme. Int J Mol Sci. 2019;20(21). doi:10.3390/ijms20215347 Cited in: PubMed; PMID 31661771.

26. Carson MJ, Doose JM, Melchior B, Schmid CD, Ploix CC. CNS immune privilege: hiding in plain sight. Immunol Rev. 2006;21348–65. doi:10.1111/j.1600-065X.2006.00441.x Cited in: PubMed; PMID 16972896.

27. Liddelow SA. Development of the choroid plexus and blood-CSF barrier. Front Neurosci. 2015;932. doi:10.3389/fnins.2015.00032 Cited in: PubMed; PMID 25784848.

28. van Tellingen O, Yetkin-Arik B, Gooijer MC de, Wesseling P, Wurdinger T, Vries HE de. Overcoming the blood-brain tumor barrier for effective glioblastoma treatment. Drug Resist Updat. 2015;191–12. doi:10.1016/j.drup.2015.02.002 Cited in: PubMed; PMID 25791797.

29. Sansom DM, Manzotti CN, Zheng Y. What's the difference between CD80 and CD86? Trends Immunol. 2003;24(6):314–9. doi:10.1016/s1471-4906(03)00111-x Cited in: PubMed; PMID 12810107.

30. Jaynes JM, Sable R, Ronzetti M, Bautista W, Knotts Z, Abisoye-Ogunniyan A, Li D, Calvo R, Dashnyam M, Singh A, Guerin T, White J, Ravichandran S, Kumar P, Talsania K, Chen V, Ghebremedhin A, Karanam B, Bin Salam A, Amin R, Odzorig T, Aiken T, Nguyen V, Bian Y, Zarif JC, Groot AE de, Mehta M, Fan L, Hu X, Simeonov A, Pate N, Abu-Asab M, Ferrer M, Southall N, Ock C-Y, Zhao Y, Lopez H, Kozlov S, Val N de, Yates CC, Baljinnyam B, Marugan J, Rudloff U. Mannose receptor (CD206) activation in tumor-associated macrophages enhances adaptive and innate antitumor immune responses. Sci Transl Med. 2020;12(530). doi:10.1126/scitranslmed.aax6337 Cited in: PubMed; PMID 32051227.

31. Yusuying S, Yusuyin S, Cheng X. Translocator Protein Regulate Polarization Phenotype Transformation of Microglia after Cerebral Ischemia-reperfusion Injury. Neuroscience. 2022;480203–16. doi:10.1016/j.neuroscience.2021.09.024 Cited in: PubMed; PMID 34624453.

32. Mantovani A, Sica A, Sozzani S, Allavena P, Vecchi A, Locati M. The chemokine system in diverse forms of macrophage activation and polarization. Trends Immunol. 2004;25(12):677–86. doi:10.1016/j.it.2004.09.015 Cited in: PubMed; PMID 15530839.

33. See AP, Parker JJ, Waziri A. The role of regulatory T cells and microglia in glioblastoma-associated immunosuppression. J Neurooncol. 2015;123(3):405–12. doi:10.1007/s11060-015-1849-3 Cited in: PubMed; PMID 26123363.

34. Adhikaree J, Moreno-Vicente J, Kaur AP, Jackson AM, Patel PM. Resistance Mechanisms and Barriers to Successful Immunotherapy for Treating Glioblastoma. Cells. 2020;9(2). doi:10.3390/cells9020263 Cited in: PubMed; PMID 31973059.

35. Baumeister SH, Freeman GJ, Dranoff G, Sharpe AH. Coinhibitory Pathways in Immunotherapy for Cancer. Annu Rev Immunol. 2016;34539–73. doi:10.1146/annurev-immunol-032414-112049 Cited in: PubMed; PMID 26927206.

36. Francisco LM, Salinas VH, Brown KE, Vanguri VK, Freeman GJ, Kuchroo VK, Sharpe AH. PD-L1 regulates the development, maintenance, and function of induced regulatory T cells. J Exp Med. 2009;206(13):3015–29. doi:10.1084/jem.20090847 Cited in: PubMed; PMID 20008522.

37. Wang S, Yao F, Lu X, Li Q, Su Z, Lee J-H, Wang C, Du L. Temozolomide promotes immune escape of GBM cells via upregulating PD-L1. Am J Cancer Res. 2019;9(6):1161–71. Cited in: PubMed; PMID 31285949.

38. Garcia-Diaz A, Shin DS, Moreno BH, Saco J, Escuin-Ordinas H, Rodriguez GA, Zaretsky JM, Sun L, Hugo W, Wang X, Parisi G, Saus CP, Torrejon DY, Graeber TG, Comin-Anduix B, Hu-Lieskovan S, Damoiseaux R, Lo RS, Ribas A. Interferon Receptor Signaling Pathways Regulating PD-L1 and PD-L2 Expression. Cell Rep. 2017;19(6):1189–201. doi:10.1016/j.celrep.2017.04.031 Cited in: PubMed; PMID 28494868.

39. Lim S-O, Li C-W, Xia W, Cha J-H, Chan L-C, Wu Y, Chang S-S, Lin W-C, Hsu J-M, Hsu Y-H, Kim T, Chang W-C, Hsu JL, Yamaguchi H, Ding Q, Wang Y, Yang Y, Chen C-H, Sahin AA, Yu D, Hortobagyi GN, Hung M-C. Deubiquitination and Stabilization of PD-L1 by CSN5. Cancer Cell. 2016;30(6):925–39. doi:10.1016/j.ccell.2016.10.010 Cited in: PubMed; PMID 27866850.

40. Sun C, Mezzadra R, Schumacher TN. Regulation and Function of the PD-L1 Checkpoint. Immunity. 2018;48(3):434–52. doi:10.1016/j.immuni.2018.03.014 Cited in: PubMed; PMID 29562194.

41. Deng L, Zhai X, Liang P, Cui H. Overcoming TRAIL Resistance for Glioblastoma Treatment. Biomolecules. 2021;11(4). doi:10.3390/biom11040572 Cited in: PubMed; PMID 33919846.

42. Karstedt S v., Montinaro A, Walczak H. Exploring the TRAILs less travelled: TRAIL in cancer biology and therapy. Nat Rev Cancer. 2017;17(6):352–66. doi:10.1038/nrc.2017.28 Cited in: PubMed; PMID 28536452.

43. Li Y-C, Tzeng C-C, Song JH, Tsia F-J, Hsieh L-J, Liao S-J, Tsai C-H, van Meir EG, Hao C, Lin C-C. Genomic alterations in human malignant glioma cells associate with the cell resistance to the combination treatment with tumor necrosis factor-related apoptosis-inducing ligand and chemotherapy. Clin Cancer Res. 2006;12(9):2716–29. doi:10.1158/1078-0432.CCR-05-1980 Cited in: PubMed; PMID 16675563.

44. Kuijlen JMA, Bremer E, Mooij JJA, Dunnen WFA den, Helfrich W. Review: on TRAIL for malignant glioma therapy? Neuropathol Appl Neurobiol. 2010;36(3):168–82. doi:10.1111/j.1365-2990.2010.01069.x Cited in: PubMed; PMID 20102513.

45. Safa AR. c-FLIP, a master anti-apoptotic regulator. Exp Oncol. 2012;34(3):176–84. Cited in: PubMed; PMID 23070002.

46. Nagane M, Cavenee WK, Shiokawa Y. Synergistic cytotoxicity through the activation of multiple apoptosis pathways in human glioma cells induced by combined treatment with ionizing radiation and tumor necrosis factor-related apoptosis-inducing ligand. J Neurosurg. 2007;106(3):407–16. doi:10.3171/jns.2007.106.3.407 Cited in: PubMed; PMID 17367063.

47. Nagane M, Pan G, Weddle JJ, Dixit VM, Cavenee WK, Huang HJ. Increased death receptor 5 expression by chemotherapeutic agents in human gliomas causes synergistic cytotoxicity with tumor necrosis factor-related apoptosis-inducing ligand in vitro and in vivo. Cancer Res. 2000;60(4):847–53. Cited in: PubMed; PMID 10706092.

48. Cuevas LM, Daud AI. Immunotherapy for melanoma. Semin Cutan Med Surg. 2018;37(2):127–31. doi:10.12788/j.sder.2018.028 Cited in: PubMed; PMID 30040090.

49. Alexander M, Kim SY, Cheng H. Update 2020: Management of Non-Small Cell Lung Cancer. Lung. 2020;198(6):897–907. doi:10.1007/s00408-020-00407-5 Cited in: PubMed; PMID 33175991.

50. Klausen U, Jørgensen NGD, Grauslund JH, Holmström MO, Andersen MH. Cancer immune therapy for lymphoid malignancies: recent advances. Semin Immunopathol. 2019;41(1):111–24. doi:10.1007/s00281-018-0696-7 Cited in: PubMed; PMID 30006739.

51. Krummel MF, Allison JP. CD28 and CTLA-4 have opposing effects on the response of T cells to stimulation. J Exp Med. 1995;182(2):459–65. doi:10.1084/jem.182.2.459 Cited in: PubMed; PMID 7543139.

52. Reardon DA, Brandes AA, Omuro A, Mulholland P, Lim M, Wick A, Baehring J, Ahluwalia MS, Roth P, Bähr O, Phuphanich S, Sepulveda JM, Souza P de, Sahebjam S, Carleton M, Tatsuoka K, Taitt C, Zwirtes R, Sampson J, Weller M. Effect of Nivolumab vs Bevacizumab in Patients With Recurrent Glioblastoma: The CheckMate 143 Phase 3 Randomized Clinical Trial. JAMA Oncol. 2020;6(7):1003–10. doi:10.1001/jamaoncol.2020.1024 Cited in: PubMed; PMID 32437507.

53. Bausart M, Préat V, Malfanti A. Immunotherapy for glioblastoma: the promise of combination strategies. J Exp Clin Cancer Res. 2022;41(1):35. doi:10.1186/s13046-022-02251-2 Cited in: PubMed; PMID 35078492.

54. Weller M, Lim M, Idbaih A, Steinbach J, Finocchiaro G, Raval R, Ashby L, Ansstas G, Baehring J, Taylor J, Honnorat J, Petrecca K, Vos F de, Wick A, Sumrall A, Roberts M, Slepetis R, Warad D, Lee M, Reardon D, Omuro A. CTIM-25. A RANDOMIZED PHASE 3 STUDY OF NIVOLUMAB OR PLACEBO COMBINED WITH RADIOTHERAPY PLUS TEMOZOLOMIDE IN PATIENTS WITH NEWLY DIAGNOSED GLIOBLASTOMA WITH METHYLATED MGMT PROMOTER: CHECKMATE 548. Neuro Oncol. 2021;23(Suppl 6):vi55-6. doi:10.1093/neuonc/noab196.217

55. Wang X, Guo G, Guan H, Yu Y, Lu J, Yu J. Challenges and potential of PD-1/PD-L1 checkpoint blockade immunotherapy for glioblastoma. J Exp Clin Cancer Res. 2019;38(1):87. doi:10.1186/s13046-019-1085-3 Cited in: PubMed; PMID 30777100.

56. Filette J de, Andreescu CE, Cools F, Bravenboer B, Velkeniers B. A Systematic Review and Meta-Analysis of Endocrine-Related Adverse Events Associated with Immune Checkpoint Inhibitors. Horm Metab Res. 2019;51(3):145–56. doi:10.1055/a-0843-3366 Cited in: PubMed; PMID 30861560.

57. Veenman L, Papadopoulos V, Gavish M. Channel-like functions of the 18-kDa translocator protein (TSPO): regulation of apoptosis and steroidogenesis as part of the host-defense response. Curr Pharm Des. 2007;13(23):2385–405. doi:10.2174/138161207781368710 Cited in: PubMed; PMID 17692008.

58. Shoshan-Barmatz V, Pittala S, Mizrachi D. VDAC1 and the TSPO: Expression, Interactions, and Associated Functions in Health and Disease States. Int J Mol Sci. 2019;20(13). doi:10.3390/ijms20133348 Cited in: PubMed; PMID 31288390.

59. Zeno S, Veenman L, Katz Y, Bode J, Gavish M, Zaaroor M. The 18 kDa mitochondrial translocator protein (TSPO) prevents accumulation of protoporphyrin IX. Involvement of reactive oxygen species (ROS). Curr Mol Med. 2012;12(4):494–501. doi:10.2174/1566524011207040494 Cited in: PubMed; PMID 22376065.

60. Casanova-González MJ, Trapero-Marugán M, Jones EA, Moreno-Otero R. Liver disease and erythropoietic protoporphyria: a concise review. World J Gastroenterol. 2010;16(36):4526–31. doi:10.3748/wjg.v16.i36.4526 Cited in: PubMed; PMID 20857522.

61. Cai L, Kirchleitner SV, Zhao D, Li M, Tonn J-C, Glass R, Kälin RE. Glioblastoma Exhibits Inter-Individual Heterogeneity of TSPO and LAT1 Expression in Neoplastic and Parenchymal Cells. Int J Mol Sci. 2020;21(2). doi:10.3390/ijms21020612 Cited in: PubMed; PMID 31963507.

62. Miettinen H, Kononen J, Haapasalo H, Helén P, Sallinen P, Harjuntausta T, Helin H, Alho H. Expression of peripheral-type benzodiazepine receptor and diazepam binding inhibitor in human astrocytomas: relationship to cell proliferation. Cancer Res. 1995;55(12):2691–5. Cited in: PubMed; PMID 7780986.

63. Cui Y, Liang Y, Ip MSM, Mak JCW. Cigarette smoke induces apoptosis via 18 kDa translocator protein in human bronchial epithelial cells. Life Sci. 2021;265118862. doi:10.1016/j.lfs.2020.118862 Cited in: PubMed; PMID 33301812.

64. Folkersma H, Boellaard R, Yaqub M, Kloet RW, Windhorst AD, Lammertsma AA, Vandertop WP, van Berckel BNM. Widespread and prolonged increase in (R)-(11)C-PK11195 binding after traumatic brain injury. J Nucl Med. 2011;52(8):1235–9. doi:10.2967/jnumed.110.084061 Cited in: PubMed; PMID 21764792.

65. Tai YF, Pavese N, Gerhard A, Tabrizi SJ, Barker RA, Brooks DJ, Piccini P. Imaging microglial activation in Huntington's disease. Brain Res Bull. 2007;72(2-3):148–51. doi:10.1016/j.brainresbull.2006.10.029 Cited in: PubMed; PMID 17352938.

66. Boutin H, Prenant C, Maroy R, Galea J, Greenhalgh AD, Smigova A, Cawthorne C, Julyan P, Wilkinson SM, Banister SD, Brown G, Herholz K, Kassiou M, Rothwell NJ. 18FDPA-714: direct comparison with 11CPK11195 in a model of cerebral ischemia in rats. PLoS One. 2013;8(2):e56441. doi:10.1371/journal.pone.0056441 Cited in: PubMed; PMID 23418569.

67. Zhang L, Hu K, Shao T, Hou L, Zhang S, Ye W, Josephson L, Meyer JH, Zhang M-R, Vasdev N, Wang J, Xu H, Wang L, Liang SH. Recent developments on PET radiotracers for TSPO and their applications in neuroimaging. Acta Pharm Sin B. 2021;11(2):373–93. doi:10.1016/j.apsb.2020.08.006 Cited in: PubMed; PMID 33643818.

68. Yousefi OS, Wilhelm T, Maschke-Neuß K, Kuhny M, Martin C, Molderings GJ, Kratz F, Hildenbrand B, Huber M. The 1,4-benzodiazepine Ro5-4864 (4-chlorodiazepam) suppresses multiple pro-inflammatory mast cell effector functions. Cell Commun Signal. 2013;11(1):13. doi:10.1186/1478-811X-11-13 Cited in: PubMed; PMID 23425659.

69. Desai R, East DA, Hardy L, Faccenda D, Rigon M, Crosby J, Alvarez MS, Singh A, Mainenti M, Hussey LK, Bentham R, Szabadkai G, Zappulli V, Dhoot GK, Romano LE, Xia D, Coppens I, Hamacher-Brady A, Chapple JP, Abeti R, Fleck RA, Vizcay-Barrena G, Smith K, Campanella M. Mitochondria form contact sites with the nucleus to couple prosurvival retrograde response. Sci Adv. 2020;6(51). doi:10.1126/sciadv.abc9955 Cited in: PubMed; PMID 33355129.

70. Elmore S. Apoptosis: a review of programmed cell death. Toxicol Pathol. 2007;35(4):495–516. doi:10.1080/01926230701320337 Cited in: PubMed; PMID 17562483.

71. Palzur E, Edelman D, Sakas R, Soustiel JF. Etifoxine Restores Mitochondrial Oxidative Phosphorylation and Improves Cognitive Recovery Following Traumatic Brain Injury. Int J Mol Sci. 2021;22(23). doi:10.3390/ijms222312881 Cited in: PubMed; PMID 34884686.

72. Menevse AN, Ammer L-M, Vollmann-Zwerenz A, Kupczyk M, Lorenz J, Weidner L, Hussein A, Sax J, Mühlbauer J, Heuschneider N, Rohrmus C, Mai LS, Jachnik B, Stamova S, Volpin V, Durst FC, Sorrentino A, Xydia M, Milenkovic VM, Bader S, Braun FK, Wetzel C, Albert NL, Tonn J-C, Bartenstein P, Proescholdt M, Schmidt NO, Linker RA, Riemenschneider MJ, Beckhove P, Hau P. TSPO acts as an immune resistance gene involved in the T cell mediated immune control of glioblastoma. Acta Neuropathol Commun. 2023;11(1):75. doi:10.1186/s40478-023-01550-9 Cited in: PubMed; PMID 37158962.

73. Raskov H, Orhan A, Christensen JP, Gögenur I. Cytotoxic CD8+ T cells in cancer and cancer immunotherapy. Br J Cancer. 2021;124(2):359–67. doi:10.1038/s41416-020-01048-4 Cited in: PubMed; PMID 32929195.

74. Li L-J, Chang PM-H, Li C-H, Chang Y-C, Lai T-C, Su C-Y, Chen C-L, Chang W-M, Hsiao M, Feng S-W. FAS receptor regulates NOTCH activity through ERK-JAG1 axis activation and controls oral cancer stemness ability and pulmonary metastasis. Cell Death Discov. 2022;8(1):101. doi:10.1038/s41420-022-00899-5 Cited in: PubMed; PMID 35249111.

75. Wu W, Klockow JL, Zhang M, Lafortune F, Chang E, Jin L, Wu Y, Daldrup-Link HE. Glioblastoma multiforme (GBM): An overview of current therapies and mechanisms of resistance. Pharmacol Res. 2021;171105780. doi:10.1016/j.phrs.2021.105780 Cited in: PubMed; PMID 34302977.

76. Woroniecka K, Chongsathidkiet P, Rhodin K, Kemeny H, Dechant C, Farber SH, Elsamadicy AA, Cui X, Koyama S, Jackson C, Hansen LJ, Johanns TM, Sanchez-Perez L, Chandramohan V, Yu Y-RA, Bigner DD, Giles A, Healy P, Dranoff G, Weinhold KJ, Dunn GP, Fecci PE. T-Cell Exhaustion Signatures Vary with Tumor Type and Are Severe in Glioblastoma. Clin Cancer Res. 2018;24(17):4175–86. doi:10.1158/1078-0432.CCR-17-1846 Cited in: PubMed; PMID 29437767.

77. Cenerenti M, Saillard M, Romero P, Jandus C. The Era of Cytotoxic CD4 T Cells. Front Immunol. 2022;13867189. doi:10.3389/fimmu.2022.867189 Cited in: PubMed; PMID 35572552.

78. Vlodavsky E, Soustiel JF. Immunohistochemical expression of peripheral benzodiazepine receptors in human astrocytomas and its correlation with grade of malignancy, proliferation, apoptosis and survival. J Neurooncol. 2007;81(1):1–7. doi:10.1007/s11060-006-9199-9 Cited in: PubMed; PMID 16868661.

79. Carpentier I, Coornaert B, Beyaert R. Function and regulation of tumor necrosis factor receptor type 2. Curr Med Chem. 2004;11(16):2205–12. doi:10.2174/0929867043364694 Cited in: PubMed; PMID 15279559.

80. Nomelini RS, Borges Júnior LE, Lima CA de, Chiovato AFC, Micheli DC, Tavares-Murta BM, Murta EFC. TNF-R2 in tumor microenvironment as prognostic factor in epithelial ovarian cancer. Clin Exp Med. 2018;18(4):547–54. doi:10.1007/s10238-018-0508-3 Cited in: PubMed; PMID 29802567.

81. Zong H, Parada LF, Baker SJ. Cell of origin for malignant gliomas and its implication in therapeutic development. Cold Spring Harb Perspect Biol. 2015;7(5). doi:10.1101/cshperspect.a020610 Cited in: PubMed; PMID 25635044.

82. DeCordova S, Shastri A, Tsolaki AG, Yasmin H, Klein L, Singh SK, Kishore U. Molecular Heterogeneity and Immunosuppressive Microenvironment in Glioblastoma. Front Immunol. 2020;111402. doi:10.3389/fimmu.2020.01402 Cited in: PubMed; PMID 32765498.

83. Bhat KPL, Balasubramaniyan V, Vaillant B, Ezhilarasan R, Hummelink K, Hollingsworth F, Wani K, Heathcock L, James JD, Goodman LD, Conroy S, Long L, Lelic N, Wang S, Gumin J, Raj D, Kodama Y, Raghunathan A, Olar A, Joshi K, Pelloski CE, Heimberger A, Kim SH, Cahill DP, Rao G, Dunnen WFA den, Boddeke HWGM, Phillips HS, Nakano I, Lang FF, Colman H, Sulman EP, Aldape K. Mesenchymal differentiation mediated by NF-κB promotes radiation resistance in glioblastoma. Cancer

Cell. 2013;24(3):331–46. doi:10.1016/j.ccr.2013.08.001 Cited in: PubMed; PMID 23993863.

84. Verhaak RGW, Hoadley KA, Purdom E, Wang V, Qi Y, Wilkerson MD, Miller CR, Ding L, Golub T, Mesirov JP, Alexe G, Lawrence M, O'Kelly M, Tamayo P, Weir BA, Gabriel S, Winckler W, Gupta S, Jakkula L, Feiler HS, Hodgson JG, James CD, Sarkaria JN, Brennan C, Kahn A, Spellman PT, Wilson RK, Speed TP, Gray JW, Meyerson M, Getz G, Perou CM, Hayes DN. Integrated genomic analysis identifies clinically relevant subtypes of glioblastoma characterized by abnormalities in PDGFRA, IDH1, EGFR, and NF1. Cancer Cell. 2010;17(1):98–110. doi:10.1016/j.ccr.2009.12.020 Cited in: PubMed; PMID 20129251.

85. Qian J, Wang C, Wang B, Yang J, Wang Y, Luo F, Xu J, Zhao C, Liu R, Chu Y. The IFN-γ/PD-L1 axis between T cells and tumor microenvironment: hints for glioma anti-PD-1/PD-L1 therapy. J Neuroinflammation. 2018;15(1):290. doi:10.1186/s12974-018-1330-2 Cited in: PubMed; PMID 30333036.

86. Taube JM, Anders RA, Young GD, Xu H, Sharma R, McMiller TL, Chen S, Klein AP, Pardoll DM, Topalian SL, Chen L. Colocalization of inflammatory response with B7-h1 expression in human melanocytic lesions supports an adaptive resistance mechanism of immune escape. Sci Transl Med. 2012;4(127):127ra37. doi:10.1126/scitranslmed.3003689 Cited in: PubMed; PMID 22461641.

87. McFarland BC, Hong SW, Rajbhandari R, Twitty GB, Gray GK, Yu H, Benveniste EN, Nozell SE. NF-κB-induced IL-6 ensures STAT3 activation and tumor aggressiveness in glioblastoma. PLoS One. 2013;8(11):e78728. doi:10.1371/journal.pone.0078728 Cited in: PubMed; PMID 24244348.

88. Leidgens V, Proske J, Rauer L, Moeckel S, Renner K, Bogdahn U, Riemenschneider MJ, Proescholdt M, Vollmann-Zwerenz A, Hau P, Seliger C. Stattic and metformin inhibit brain tumor initiating cells by reducing STAT3-phosphorylation. Oncotarget. 2017;8(5):8250–63. doi:10.18632/oncotarget.14159 Cited in: PubMed; PMID 28030813.

89. Fierro J, DiPasquale J, Perez J, Chin B, Chokpapone Y, Tran AM, Holden A, Factoriza C, Sivagnanakumar N, Aguilar R, Mazal S, Lopez M, Dou H. Dual-sgRNA CRISPR/Cas9 knockout of PD-L1 in human U87 glioblastoma tumor cells inhibits proliferation, invasion, and tumor-associated macrophage polarization. Sci Rep. 2022;12(1):2417. doi:10.1038/s41598-022-06430-1 Cited in: PubMed; PMID 35165339.

90. Issop L, Ostuni MA, Lee S, Laforge M, Péranzi G, Rustin P, Benoist J-F, Estaquier J, Papadopoulos V, Lacapère J-J. Translocator Protein-Mediated Stabilization of Mitochondrial Architecture during Inflammation Stress in Colonic Cells. PLoS One. 2016;11(4):e0152919. doi:10.1371/journal.pone.0152919 Cited in: PubMed; PMID 27054921.

91. Akyuva Y, Nazıroğlu M, Yıldızhan K. Selenium prevents interferon-gamma induced activation of TRPM2 channel and inhibits inflammation, mitochondrial oxidative stress, and apoptosis in microglia. Metab Brain Dis. 2021;36(2):285–98. doi:10.1007/s11011-020-00624-0 Cited in: PubMed; PMID 33044639.

92. Lue LF, Rydel R, Brigham EF, Yang LB, Hampel H, Murphy GM, Brachova L, Yan SD, Walker DG, Shen Y, Rogers J. Inflammatory repertoire of Alzheimer's disease and nondemented elderly microglia in vitro. Glia. 2001;35(1):72–9. doi:10.1002/glia.1072 Cited in: PubMed; PMID 11424194.

93. Beckers L, Ory D, Geric I, Declercq L, Koole M, Kassiou M, Bormans G, Baes M. Increased Expression of Translocator Protein (TSPO) Marks Pro-inflammatory Microglia but Does Not Predict Neurodegeneration. Mol Imaging Biol. 2018;20(1):94–102. doi:10.1007/s11307-017-1099-1 Cited in: PubMed; PMID 28695372.

94. Zhou D, Ji L, Chen Y. TSPO Modulates IL-4-Induced Microglia/Macrophage M2 Polarization via PPAR-γ Pathway. J Mol Neurosci. 2020;70(4):542–9. doi:10.1007/s12031-019-01454-1 Cited in: PubMed; PMID 31879837.

95. Lohr J, Ratliff T, Huppertz A, Ge Y, Dictus C, Ahmadi R, Grau S, Hiraoka N, Eckstein V, Ecker RC, Korff T, Deimling A v., Unterberg A, Beckhove P, Herold-Mende C. Effector T-cell infiltration positively impacts survival of glioblastoma patients and is impaired by tumor-derived TGF-β. Clin Cancer Res. 2011;17(13):4296–308. doi:10.1158/1078-0432.CCR-10-2557 Cited in: PubMed; PMID 21478334.

96. Song Y, Chen Y, Li Y, Lyu X, Cui J, Cheng Y, Zhao L, Zhao G. Metformin inhibits TGF-β1-induced epithelial-to-mesenchymal transition-like process and stem-like properties in GBM via AKT/mTOR/ZEB1 pathway. Oncotarget. 2018;9(6):7023–35. doi:10.18632/oncotarget.23317 Cited in: PubMed; PMID 29467947.

97. Trickett A, Kwan YL. T cell stimulation and expansion using anti-CD3/CD28 beads. J Immunol Methods. 2003;275(1-2):251–5. doi:10.1016/s0022-1759(03)00010-3 Cited in: PubMed; PMID 12667688.

98. van Roosmalen IAM, Reis CR, Setroikromo R, Yuvaraj S, Joseph JV, Tepper PG, Kruyt FAE, Quax WJ. The ER stress inducer DMC enhances TRAIL-induced apoptosis in glioblastoma. Springerplus. 2014;3(1):495. doi:10.1186/2193-1801-3-495 Cited in: PubMed; PMID 26331107.

99. Zeno S, Zaaroor M, Leschiner S, Veenman L, Gavish M. CoCl(2) induces apoptosis via the 18 kDa translocator protein in U118MG human glioblastoma cells. Biochemistry. 2009;48(21):4652–61. doi:10.1021/bi900064t Cited in: PubMed; PMID 19358520.

100. Motaln H, Koren A, Gruden K, Ramšak Ž, Schichor C, Lah TT. Heterogeneous glioblastoma cell cross-talk promotes phenotype alterations and enhanced drug resistance. Oncotarget. 2015;6(38):40998–1017. doi:10.18632/oncotarget.5701 Cited in: PubMed; PMID 26517510.

101. Bonsack F, Sukumari-Ramesh S. TSPO: An Evolutionarily Conserved Protein with Elusive Functions. Int J Mol Sci. 2018;19(6). doi:10.3390/ijms19061694 Cited in: PubMed; PMID 29875327.

102. Hu B, Zhong L, Weng Y, Peng L, Huang Y, Zhao Y, Liang X-J. Therapeutic siRNA: state of the art. Signal Transduct Target Ther. 2020;5(1):101. doi:10.1038/s41392-020-0207-x Cited in: PubMed; PMID 32561705.

103. Haasnoot J, Westerhout EM, Berkhout B. RNA interference against viruses: strike and counterstrike. Nat Biotechnol. 2007;25(12):1435–43. doi:10.1038/nbt1369 Cited in: PubMed; PMID 18066040.

104. Sudbery I, Enright AJ, Fraser AG, Dunham I. Systematic analysis of off-target effects in an RNAi screen reveals microRNAs affecting sensitivity to TRAIL-induced apoptosis. BMC Genomics. 2010;11175. doi:10.1186/1471-2164-11-175 Cited in: PubMed; PMID 20230625.

105. Volpin V, Michels T, Sorrentino A, Menevse AN, Knoll G, Ditz M, Milenkovic VM, Chen C-Y, Rathinasamy A, Griewank K, Boutros M, Haferkamp S, Berneburg M, Wetzel CH, Seckinger A, Hose D, Goldschmidt H, Ehrenschwender M, Witzens-Harig M, Szoor A, Vereb G, Khandelwal N, Beckhove P. CAMK1D Triggers Immune Resistance of Human Tumor Cells Refractory to Anti-PD-L1 Treatment. Cancer Immunol Res. 2020;8(9):1163–79. doi:10.1158/2326-6066.CIR-19-0608 Cited in: PubMed; PMID 32665263.

106. Zhong B, Liu M, Bai C, Ruan Y, Wang Y, Qiu L, Hong Y, Wang X, Li L, Li B. Caspase-8 Induces Lysosome-Associated Cell Death in Cancer Cells. Mol Ther. 2020;28(4):1078–91. doi:10.1016/j.ymthe.2020.01.022 Cited in: PubMed; PMID 32053770.

107. Han J-H, Park J, Kang T-B, Lee K-H. Regulation of Caspase-8 Activity at the Crossroads of Pro-Inflammation and Anti-Inflammation. Int J Mol Sci. 2021;22(7). doi:10.3390/ijms22073318 Cited in: PubMed; PMID 33805003.

9 Abbreviations

5-ALA	5-aminolevulinic acid
ANT	Adenine Nucleotide Transporter
AP1	Activator Protein 1
Apaf-1	Apoptotic Protease Activating Factor 1
APC	Allophycocyanin; antigen presenting cell
ATP	Adenosine triphosphate
Bax	Bcl-2-associated X protein
BBB	blood brain barrier
Bcl-2	B cell lymphoma 2
BTIC	Brain Tumor Initiating Cells
BV421	brilliant violet 421 dye
CAMK1D	Calcium/Calmodulin-dependent protein kinase 1D
Cas9	CRISPR associated protein 9
CBR	central benzodiazepine receptor
CD	cluster of differentiation
cDNA	complementary DNA
c-FLIP	Casp8 and FADD-like apoptosis regulator
CI	confidence interval
CIRI	cerebral ischemia-reperfusion injury
CLL	chronic lymphocytic leukemia
CLM	complete lymphocyte medium
CMV	Cytomegalovirus
CNS	central nervous system
CO_2	carbon dioxide
COP9	constitutive photomorphogenesis 9
$CoCl_2$	cobalt dichloride
CSF	cerebrospinal fluid
CSN5	COP 9 signalosome complex subunit 5
CRISPR	clustered regularly interspaced short palindromic repeats
CTLA-4	cytotoxic T lymphocyte-associated protein 4
DC	dentritic cell
DISC	death-inducing signaling complex

DMEM	dulbecco’s modified eagle medium
DMSO	dimethyl sulfoxide
DNA	deoxyribonucleic acid
DPA-714	*N*,*N*-diethyl-2-[4-(2-fluoroethoxy)phenyl]-5,7-dimethylpyrazolo[1,5-*a*]pyrimidine-3-acetamide
DR	death receptor
EDTA	ethylenediaminetetraacetic acid
EGF	endothelial growth factor
EGFRvIII	EGF receptor variant III
ELISA	Enzyme-linked immunosorbent Assay
EMT	epithelial-mesenchymal-transition
ERK	extracellular signal-regulated kinase
FACS	fluorescent-activated cell sorting
FADD	Fas-associated death domain protein
Fas	FS-7-associated surface antigen
FasL	Fas ligand
FCS	fetal calf serum
FGF	fibroblast growth factor
FGIN-1-27	2-(4-Flurophenyl)-*N,N*-dihexyl-1*H*-indole-3-acetamide
FITC	Fluorescein-5-isothiocyanate
FluTC	cytotoxic Flu T cell
GABA	gamma-aminobutyric acid
GBM	Glioblastoma multiforme
gDNAse	genomic DNAse
GEPIA	Gene Expression Profiling Interactive Analysis
GZMB	Granzyme B
H_2SO_4	sulfuric acid
HHV	human herpesvirus
HLA	Human Leukocyte Antigen
HMG-CoA	3-hydroxy-3-methyl-glutaryl-coenzyme A reductase
HRP	horseradish peroxidase
IBP	isoquinoline binding protein
ICI	Immune checkpoint inhibitor
IDH	Isocitrate dehydrogenase

IDO	Indolamin-2,3-Dioxygenase
IFNγ	Interferon gamma
IFNG-R1	Interferon gamma receptor 1
IgG	Immunoglobulin G
IL	Interleukin
IMM	inner mitochondrial membrane
IRF	Interferon regulatory factor
iTME	immune tumor microenvironment
ITSM	immunoreceptor tyrosine-based switch motif
JAK	Janus kinase
JNK	c-Jun N-terminal kinase
kd	knock-down
ko	knock-out
LDL	low density lipoprotein
LGG	lower grade glioma
LOH	loss of heterozygosity
LPS	lipopolysaccharide
MEK	Mitogen-activated protein kinase kinase
MES	mesenchymal
MGMT	O-6-methylguanine-DNA methyltransferase
MHC	major histocompatibility complex
miRNA	micro RNA
mOS	mean overall survival
mPTP	mitochondrial permeability transition pore
MRI	Magnetic Resonance Imaging
mRNA	messenger RNA
MUT	mutated; mutation
My88	myeloid differentiation primary response 88
NF-κB	nuclear factor kappa-light-chain-enhancer of activated B cells
NSCLC	non small cell lung cancer
OD	optical density
OKT3	Muromonab-CD3
OMM	outer mitochondrial membrane
OPC	oligodendrocyte precursor cells

PAMPs	pathogen-associated molecular patterns
PBMC	peripheral blood mononuclear cells
PBR	peripheral benzodiazepine receptor
PBS-T	phosphate buffered saline – tween
PD-1	Programmed Death 1
PDGF-R	platelet derived growth factor receptor
PD-L1 (CD274)	Programmed Death ligand 1
PE	Phycoerythrin
PerCP-Cy5.5	Peridinin chlorophyll cyanin 5.5
PET	Positron Emission Tomography
PGE2	Prostaglandin E2
PK 11195	*N*-Butan-2-yl-1-(2-chlorophenyl)-*N*-methylisoquinoline-3-carboxamide
PKC	Protein kinase C
PMS	phenazine methosulfate
PMT	proneural-mesenchymal transition
PN	proneural
PPIX	Protoporphyrin IX
PRF1	Perforin-1
qPCR	quantitative polymerase chain reaction
REP	rapid expansion protocol
RISC	RNA-induced silencing complex
RLU	relative luminescence unit
RNA	ribonucleic acid
RNAi	RNA interference
Ro5-4864	4'-chlorodiazepam
ROS	reactive oxygen species
RT	radiotherapy
RT-qPCR	reverse transcription quantitative polymerase chain reaction
Scr	scrambled sequence
SD	standard deviation
SHP-2	Src homology region 2 domain-containing phosphatase-2
siRNA	small interfering RNA
SOC	standard of care

STAT	signal transducer and activator of transcription
TAM	tumor-associated macrophage
TCR	T cell receptor
TGFβ	tumor growth factor beta
Th17	T helper 17 cell
TIL	tumor-infiltrating lymphocyte
TLR	toll-like receptor
TMZ	Temozolomide
TNFα	tumor necrosis factor alpha
TNF-R	TNF receptor
TNFRSF	TNF receptor superfamily
TP53	tumor protein p53, transformation-related protein 53
TPM	transcripts per million
TRAF	TNF receptor associated factor
TRAIL	tumor necrosis factor related apoptosis inducing ligand
Treg	regulatory T cell
TSPO	translocator protein 18 kDa
VDAC	voltage-dependent anion channel
VEGF	vascular endothelial growth factor
WHO	World Health Organization
WT	wildtype

Erklärung

Ich erkläre hiermit, dass ich die vorliegende Arbeit ohne unzulässige Hilfe Dritter und ohne Benutzung anderer als der angegebenen Hilfsmittel angefertigt habe. Die aus anderen Quellen direkt oder indirekt übernommenen Daten und Konzepte sind unter Angabe der Quelle gekennzeichnet. Insbesondere habe ich nicht die entgeltliche Hilfe von Vermittlungs- bzw. Beratungsdiensten (Promotionsberater oder andere Personen) in Anspruch genommen. Niemand hat von mir unmittelbar oder mittelbar geldwerte Leistungen für Arbeit erhalten, die im Zusammenhang mit dem Inhalt der vorgelegten Dissertation stehen. Die Arbeit wurde bisher weder im In- noch im Ausland in gleicher oder ähnlicher Form einer anderen Prüfungsbehörde vorgelegt.

Regensburg, 14.03.2024

10 Danksagung

Zuallererst möchte ich Herrn Prof. Beckhove für die schnelle und unkomplizierte Möglichkeit danken, am LIT meine Doktorarbeit anfertigen zu können. Durch seine Erfahrung und Kompetenz wurde ich nicht nur motiviert, Theoriewissen zu vertiefen, sondern auch Ergebnisse noch kritischer zu hinterfragen. Danke auch an Sabine Termer für ihre Freundlichkeit und ihre hervorragende Organisationsfähigkeit.

Auch meiner Betreuerin Ayşe möchte ich Danke sagen für ihr Lektorat und ihre freundliche, sehr geduldige Art. Vor allem Du hast mir die Praktiken im Labor gezeigt und mir bei vielen Fragestellungen zur Seite gestanden. Deine fleißige Natur hat mich während der Laborarbeit sehr angesteckt.

Danke auch an das gesamte restliche Team für ihren zuvorkommenden Umgang mit einem Medizinstudenten mit nur wenig praktischem Vorwissen und für Eure grenzenlose Geduld.

Danke an Thomas, Marian und Severin für das zusätzliche Lektorat dieser Arbeit.

Zuletzt möchte ich meiner Freundin Charlotte und meiner Ehefrau Anneliese vor allem für ihre außerordentliche Güte und Liebe danken, die mir das Studium und diese Arbeit erst möglich gemacht haben.